

Effect of Printing Parameters on Mechanical Characteristics of 3D
Printed PLA



Author

MUHAMMAD UZAIR NADEEM

00000330022

Supervisor

Dr. HASAN AFTAB SAEED

DEPARTMENT OF MECHANICAL ENGINEERING
COLLEGE OF ELECTRICAL & MECHANICAL ENGINEERING
NATIONAL UNIVERSITY OF SCIENCES AND TECHNOLOGY
ISLAMABAD

April, 2023

Effect of Printing Parameters on Mechanical Characteristics of 3D

Printed PLA

Author

MUHAMMAD UZAIR NADEEM

00000330022

A thesis submitted in partial fulfillment of the requirements for the degree of
MS Mechanical Engineering

Thesis Supervisor:

Dr. HASAN AFTAB SAEED

Thesis Supervisor's Signature: _____

DEPARTMENT OF MECHANICAL ENGINEERING
COLLEGE OF ELECTRICAL & MECHANICAL ENGINEERING
NATIONAL UNIVERSITY OF SCIENCES AND TECHNOLOGY,
ISLAMABAD

APRIL, 2023

Declaration

I certify that this research work titled “*Effect of printing parameters on mechanical characteristics of 3D printed PLA*” is my own work. The work has not been presented elsewhere for assessment. The material that has been used from other sources it has been properly acknowledged / referred.

Signature of Student

Muhammad Uzair Nadeem

2020-NUST-MS-Mech08

Language Correctness Certificate

This thesis has been read by an English expert and is free of typing, syntax, semantic, grammatical, and spelling mistakes. The thesis is also according to the format given by the university.

Signature of Student

Muhammad Uzair Nadeem

Registration Number

00000330022

Signature of Supervisor

Copyright Statement

- Copyright in the text of this thesis rests with the student author. Copies (by any process), either in full or of extracts, may be made only in accordance with instructions given by the author and lodged in the Library of NUST College of E&ME. Details may be obtained by the Librarian. This page must form part of any such copies made. Further copies (by any process) may not be made without the permission (in writing) of the author.
- The ownership of any intellectual property rights which may be described in this thesis is vested in NUST College of E&ME, subject to any prior agreement to the contrary, and may not be made available for use by third parties without the written permission of the College of E&ME, which will prescribe the terms and conditions of any such agreement.
- Further information on the conditions under which disclosures and exploitation may take place is available from the Library of NUST College of E&ME, Rawalpindi.

Acknowledgments

I am thankful to my Creator Allah Subhana-Watala to have guided me throughout this work at every step and for every new thought which You setup in my mind to improve it. Indeed I could have done nothing without Your priceless help and guidance. Whosoever helped me throughout the course of my thesis, whether my parents or any other individual was Your will, so indeed, none be worthy of praise but You.

I am profusely thankful to my beloved parents, who raised me when I was not capable of walking and continued to support me throughout every department of my life.

I would also like to express special thanks to my supervisor Dr. Hasan Aftab Saeed, for his help throughout my thesis and also for Finite Element Methodology (FEM) course, which he has taught me. I can safely say that I haven't learned any other engineering subject in such depth as the ones which he has taught.

I would also like to pay special thanks to Dr. Bilal Anjum for his tremendous support and cooperation. Each time I got stuck in something, he came up with a solution. Without his help, I wouldn't have been able to complete my thesis. I appreciate his patience and guidance throughout the whole thesis.

I would also like to thank Dr. Rehan Khan and Dr. Naveed Akram Din for being on my thesis guidance and evaluation committee and express my special Thanks to Dr. Malik Adeel Umer (SCME) and Dr. Shoaib Butt (SCME) for their help. I am also thankful to Furqan Ahmed and Ali Imran for their support and cooperation.

Finally, I would like to express my gratitude to all the individuals who have rendered valuable assistance to my study.

*Dedicate to my exceptional parents and adored siblings whose
tremendous support and cooperation led me to this
wonderful accomplishment*

Abstract

To determine the best 3D printing settings for enhancing the mechanical characteristics of PLA that has been 3D printed, the Taguchi Design of Experiments approach was used in the study. In particular, the infill printing temperature, infill density, infill pattern, layer thickness, and post-heat treatment (annealing) temperature were optimised using the L18 orthogonal array design. A statistical method called the Taguchi Design of Experiments is used to carefully look at how various characteristics or variables impact a particular process. The L18 orthogonal array design is a type of experimental design that allows for the efficient testing of multiple factors with minimal runs. The four most important parameters: printing temperature of the infill, infill density, infill pattern and layer thickness temperature are optimized by L18 array. The optimization procedure also took post-heat treatment (annealing) temperature into account in addition to these four variables. By examining the signal-to-noise (S/N) ratio, the ideal printing parameters for the maximum tensile strength and strain percentage were identified. The desired responses were developed into a regression model. The gyroid, infill pattern, 0.16 mm layer thickness, 90% infill density, and 195 °C printing temperature were the conditions that produced the best tensile strength; however, the conditions that produced the best strain percentage were the same, with the exception of the annealing temperature. The specimen that hadn't been annealed had the highest strain percentage. Experimental validation studies were used to confirm the identified optimal conditions. The experimental results correspond with the expected values. To ascertain the effects of individual parameters and to pinpoint the most important process parameter, an analysis of variance (ANOVA) was performed. The infill pattern, infill percentage, and post-printing heat treatment temperature were all found to have significant effects on the mechanical behavior of the 3D printed PLA, according to an analysis of variance (ANOVA), whereas no variable had a significant impact on the strain percentage.

Key Words: *3D printing, Signal to noise ratio, ANOVA, printing parameters, optimal parameters*

Table of Contents

Declaration	i
Language Correctness Certificate	ii
Copyright Statement	iii
Acknowledgements	iv
Abstract	vi
Table of Contents	vii
List of Figures	viii
List of Tables	x
CHAPTER 1: INTRODUCTION	1
1.1 3D Printing Paramters:.....	5
1.2 Literature Review:	5
CHAPTER 2: METHODOLOGY	30
2.1 Material:.....	30
2.2 Selection of Parameters and levels.....	30
2.3 Sample Preparation	32
2.4 Orthogonal Array Experiment:.....	34
2.5 Annealing:.....	34
2.6 Tensile Testing	36
CHAPTER 3: RESULTS AND DISCUSSION	37
3.1 Tensile Test Results of Taguchi Matrix:	37
3.2 Signal to Noise Ratio (<i>S/N</i>):	37
3.3 Estimation of optimum parameters:.....	41
3.4 Prediction of optimum parameter by Regression equation:.....	41
3.5 Analysis of Variance (ANOVA).....	43
3.6 Validation Test:	45
CHAPTER 4: CONCLUSION AND FUTURE WORK	47
4.1 Future work:.....	458
REFERENCES	499

List of Figures

Figure 1: FDM schematic	1
Figure 2: Infill percentage	3
Figure 3: Infill patterns	4
Figure 4: Grid And triangular Infill	4
Figure 5: Tensile stress for various infill structures.....	5
Figure 6: Comparison of compression strength for 20 and 80% infill density.....	13
Figure 7: Infill patterns: (a) grid, (b) tri-hexagonal, and (c) concentric. Grid pattern infill densities: (d) 25%, (e) 50%, and (f) 75%.	15
Figure 8: Maximum ultimate tensile strength (RM) and yield strength (R02) for every infill pattern.....	16
Figure 9: Process parameters: a) Build orientation. b) Layer thickness.....	17
Figure 10: Average stress-strain curves for the tensile specimens under different printing conditions	18
Figure 11: Effects of infill pattern and infill density on the tensile strength of the 3D-printed specimens, (a) tensile strength vs. infill density and (b) tensile strength vs. infill pattern	19
Figure 12: The adopted infill patterns: (a) linear, (b) diamond, (c) hexagonal.	23
Figure 14: The stress–strain curves of eight experiments designed by the Taguchi method.	25
Figure 15: Solid works geometry of the specimen	32
Figure 17: Octet infill pattern with 70, 80 and 90% infill density	33
Figure 18: Tri-hexagonal infill pattern with 70, 80, and 90% infill density.....	33
Figure 19: Gyroid infill pattern with 70, 80 and 90% infill density	33
Figure 20: Samples placed in an oven for annealing	35
Figure 21: (a) Samples annealed at 90°C, (b) Samples annealed at 130°C.....	35
Figure 22: Tensile test of a specimen.....	36
Figure 23: (a) 90°C annealed specimen after tensile test, (b) 130°C annealed specimen after tensile test, (c) un-annealed specimen after tensile test	36
Figure 24: S/N ratio for UTS responses	39
Figure 25: Mean for UTS responses	40

Figure 26: S/N ratio for Strain percentage responses.....41

List of Tables

Table 1: Process parameters for sample preparation.....	24
Table 2: Values of process parameters	31
Table 3: Constant process parameters	31
Table 4: Taguchi orthogonal array [Infill patterns: 1(octet), 2(Tri-hexagonal), 3(Gyriod)]	33
Table 5: Experimental results of samples for Taguchi L18 Array	37
Table 6: The S/N ratio analysis for tensile test result	38
Table 7: Response table for means	39
Table 8: S/N ratio analysis for strain percentage	40
Table 9: Regression model summary	42
Table 10: Coefficients table of the regression equation for UTS	42
Table 11: Coefficient table of the regression equation for stain %	43
Table 12: Regression model summary for strain %age	43
Table 13: Optimum parameters.....	44
Table 14: Analysis of Variance (Maximum stress).....	44
Table 15: Analysis of Variance (strain %age)	45

CHAPTER 1: INTRODUCTION

A group of advanced manufacturing methods known as additive manufacturing (AM) involve building parts layer by layer. With additive manufacturing, material is added to create the desired shape as opposed to subtractive production, which involves material being removed to create parts. An additive manufacturing technique called fused deposition modelling (FDM) uses thermoplastic fibre to build parts layer by layer from 3D-CAD models in STL format. The thermoplastic fibre is heated in the FDM system to a semi-liquid state before being extruded through a tiny pin. The filament used in FDM systems typically has a circular cross-section and a particular diameter, with 1.75 mm or 3.0 mm being the most popular diameters [1].

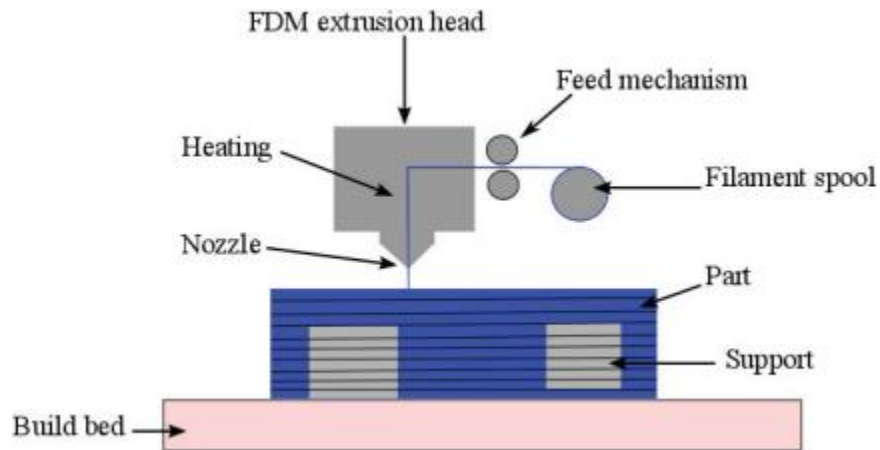


Figure 1: FDM schematic [1]

Several critical motivations exist for using additive manufacturing (3D printing) in various industries and applications. Some of the most significant benefits and drivers of additive manufacturing include customization, speed, efficiency, reduced wastage, complex geometries, lightweight and robust products, on-demand production, etc. FDM or 3D printing is the technique for manufacturing complicated designs and structures that are lighter in shape and at lower material cost because of zero wastage [2]. One of the main advantages of FDM is its capacity to produce complex shapes and designs, such as parts within parts and complex holes. FDM has a number of other advantages as well. The use of various materials with various mechanical properties and colours can also be combined into a single printed piece thanks to FDM. [3].

Currently, there are a large number of materials available for FDM printing, including polylactic acid (PLA), acrylonitrile Butadiene Styrene (ABS), Polyvinyl Alcohol (PVA), Polyethylene Ethylene terephthalate (PETG), etc. Polylactic Acid (PLA) is a thermoplastic polymer made from renewable resources, such as corn starch, sugarcane, or cassava. It is commonly used in various applications, including 3D printing, packaging, and consumer products. One of the critical advantages of PLA is that it is biodegradable and compostable, making it an environmentally friendly alternative to other types of plastic. Additionally, PLA is easy to process and has good dimensional stability, making it suitable for various applications.

When used in 3D printing, PLA is melted and extruded through a nozzle to build up the final product layer by layer. The material has a low melting temperature, is easy to work with, and produces good results with various 3D printers. PLA is also available in multiple colors and finishes, making it an attractive choice for many applications [4]. Due to its ability to create quick products, dependable prototypes, and intricate parts while being rigid yet flexible, PLA filament is a material that is frequently used in FDM systems. When compared to petrochemical-based materials, PLA is more environmentally friendly because it is made from renewable resources and environmentally friendly materials that require little energy to process [3]. Properties of the parts manufactured by FDM technology can be enhanced by varying parameters before printing or mechanical properties can be improved by post-processing, i.e., heating. The preprocessing parameters are infill density, bed temperature, infill orientation, printing speed, filament temperature, layer height, etc [4].

This technique has both advantages and disadvantages. Additive manufacturing has numerous benefits over traditional manufacturing processes. It allows for the creation of complex, customizable shapes with little to no waste of material. It also enables faster prototyping and product development and reduces the need for tooling and other specialized equipment. In addition, additive manufacturing can be used to produce products on demand without the need for large-scale manufacturing facilities. But this method is still under development as the parts produced have less tensile strength than those made conventional. This issue can be minimized by varying manufacturing parameters like layer height, infill density, printing speed, raster angle, extrusion temperature, etc. Researchers have been optimizing the best parameters for the highest tensile strength for some time. This strength can be improved by varying some parameters discussed in next section.

1.1 3D Printing Parameters:

The following are the parameters that must be addressed before printing any object on a 3D printer. These parameters can be set on Ultimaker Cura, which is connected to a 3D printer, according to desired strength, shape, and object cost. Some of them are discussed below.

1.1.1 Infill density:

It is represented as the percentage of the solid material the solid model should fill in with. To save material cost and speed up the printing time, infill density should be low, but infill density needs to be higher to achieve higher strength. Infill density cannot be 100% depending on layer angles and orientation [5].

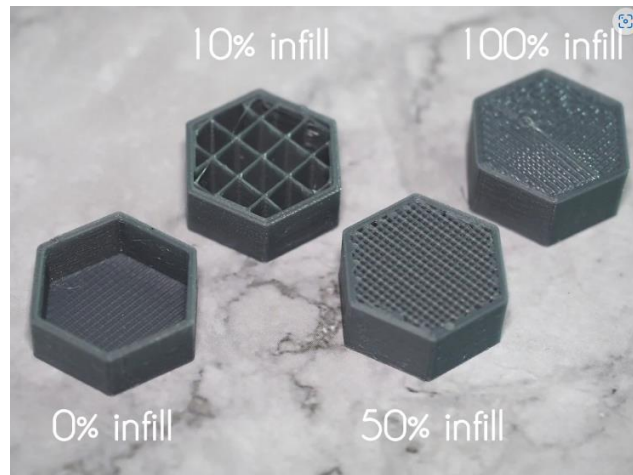


Figure 2: Infill percentage [6]

1.1.2 Layer Height:

A 3D printer layer creates an object by layer. Layer height is the number of layers used to create that object. If layer thickness is smaller, more layers are needed to complete the geometry, and thus the number of layers is increased [7].

1.1.3 Temperature:

The temperature of the filament used in the printing process is referred to as the nozzle temperature of a 3D printer. The nozzle temperature should typically be kept between 210°C and 250°C when using PLA. On the other hand, the printer's bed temperature, which refers to the temperature of the plate used to create the specimen, should be maintained at about 70°C [8].

1.1.4 Infill Orientation:

Infill orientation is the pattern with which the 3D-printed solid model is filled inside and cannot be seen from the outside. The purpose is to increase strength.

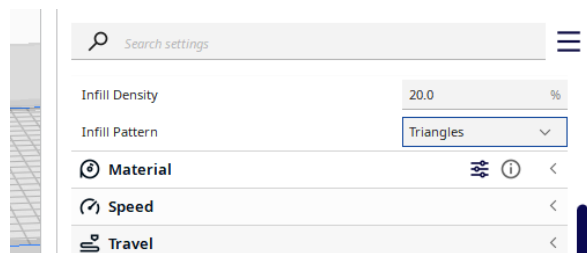


Figure 3: Infill patterns

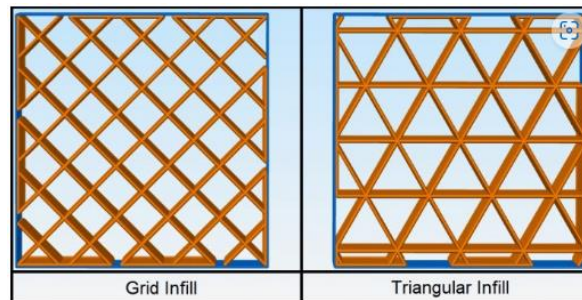


Figure 4: Grid And triangular Infill [9]

Some other parameters can also affect the properties of 3D printed PLA samples, such as; filament diameter, nozzle angle, printing speed, filament size, nozzle size, and layer thickness [10].

The strength of the 3D printed parts can be further increased by post-heating them. When compared to features that were not heat treated, the mechanical properties of the printed parts can be significantly improved by heat treatment [4].

In this study, tensile strength of 3D printed specimens, of PLA, with varying parameters is analyzed. Post-heat treatment is done on samples, and results are compared to pre-heated ones.

The Taguchi method is utilized as framework to construct and analyze the experimental design. Infill density, layer thickness, printing temperature, and least used infill shapes in the previous literature are used, annealed at different temperatures, and then UTM testing is performed to calculate tensile strength.

1.2 Literature Review:

The ideal weight, infill ratio, and infill structures for applications requiring tensile strength can be chosen based on the desired outcome, according to a study that looked at the yield strength and density ratio of infill constructions. Gyroid, rhombic, spherical, and honeycomb (hexagonal) infill patterns were designed and sliced in 3D using Autodesk Fusion 360 and Flash Print. The created specimen was tested for its tensile properties using a universal testing machine and ASTM D638 standards. The hexagonal (honeycomb) infill structure showed good tensile behaviour when compared to other infill ratios. The research also discovered that printing time increased in tandem with the infill ratio. To make up for the shortened manufacturing time, the extruder's reduced travel time resulted in a 100% infill ratio, which decreased the printing time for the specimen [11].

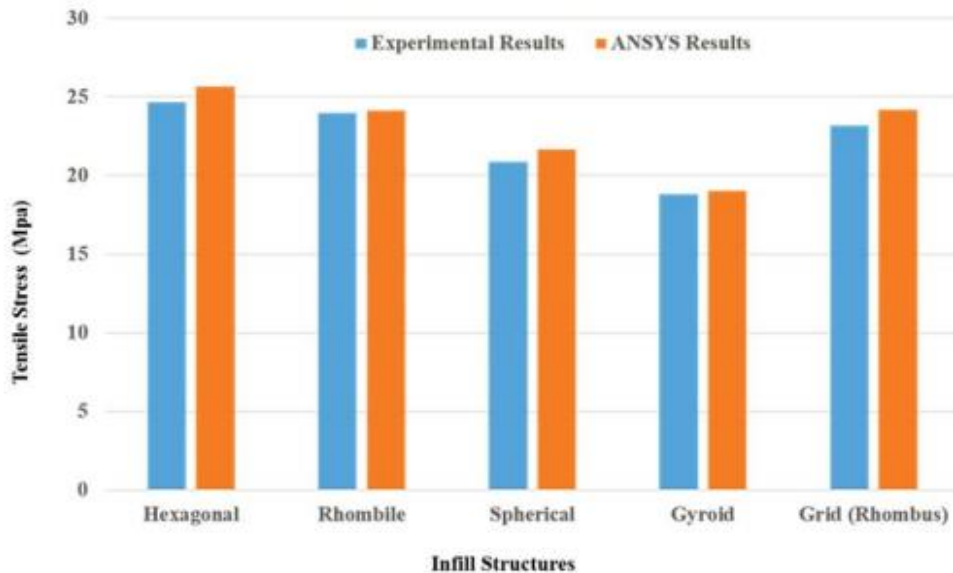


Figure 5: Tensile stress for various infill structures [11]

Another study investigated the impact of printing temperature on the tensile strength and crystallinity of PLA filament, which is used in FFF. Different PLA filament colours have a

specific crystallinity % and altering this percentage can drastically change the tensile strength of the printed objects, according to Pearce's research. The crystallinity of the PLA material improves from 190°C to 210°C, reaches its maximum, and subsequently decreases to a lower value at 215°C. The tensile strength of the printed items likewise increases as the temperature climbs from 190°C to 210°C. Surprisingly, prints made with RepRap 3-D printers can result in parts with tensile strengths that are equal to or greater than those made with prints made with proprietary 3-D printers. Additionally, all samples had an average Young's modulus of 2.78 GPa (+/- 0.35), which is within the range allowed for PLA. The hue or temperature of 3-D printed parts can be changed during printing to suit specific uses [12].

This study examined the relationship between the hardness and tensile strength of 3D-printed materials as well as the performance of the evaluated print settings. The findings indicate a significant correlation between these two variables. When printing PLA thermoplastic material using FDM technology, three processing parameters—build orientation, raster direction angle, and layer thickness—were changed. On-edge print orientation generated the highest Young's modulus, UTS, and hardness values due to its robust structure, however flat orientation was preferred for elongation at UTS and elongation at break. The chosen raster direction angle settings had no discernible effect on hardness, however a [0/45°] raster angle drastically changed the mechanical properties. Layer thickness of 0.1 mm had an effect on Shore D hardness and mechanical characteristics such as UTS, elongation at UTS, and elongation at break, however Young's modulus rose at 0.2 mm. Out of all the 3D printing process factors examined, print orientation was found to have the greatest impact on the mechanical properties of the employed PLA material. The fracture profile of the specimens following the tensile test was affected by or followed by the relatively sharp or zigzag inner structure [13].

According to a fresh study, 3D printing technology may be used to produce a variety of forms and items from 3D blueprints. This is a substantial divergence from the standard injection moulding procedure since it saves time and money and does not require expensive moulds. The capacity to utilise less material is facilitated by changes in the form requirements, internal density of 3D printers, and the 3D design of printed things. A study that looked at the tensile strength of PLA specimens made in the FDM mode found an inverse relationship between changes in interior filling density and an increase in tensile strength. The PLA specimen's linear

internal geometry provided the largest tensile elongation at the breakpoint and concentric internal geometry the best tensile strength. The direction in which the specimen was placed throughout the manufacturing process was shown to have the greatest impact on the tensile elongation at the breakpoint. This discovery shows that by adjusting the inner density and form utilising the 3D printing technology, it may be possible to alter physical attributes like tensile strength and tensile elongation at the breakpoint. The study's conclusion is that 3D printing technology has a lot of potential in terms of the forms and items it can make, as well as its ability to utilise less material, lower manufacturing costs, and free up time and resources. By altering the interior density and geometry of 3D printed items, one may improve their elongation and tensile strength at break for specific purposes [14].

This study's main objective was to determine the impact of printing speed and raster orientation on the durability of 3D-printed components. To research this association, sample coupons were printed at varied raster orientations and printing rates. The studies' findings shown that the strength of the specimens is considerably influenced by the raster orientation. The elastic modulus of the samples printed at 0° had the largest value, and it steadily fell as the raster direction rose. According to the data, the specimen printed at 80 mm/s with the 90° raster orientation had the lowest ultimate tensile strength, declining by 53.76%. In addition, the study stressed the importance of printing speed in evaluating production costs since increasing printing speed might affect printing stability and extrusion volume. The strength of the 3D-printed test coupons was also significantly impacted by the combination of raster direction and printing speed, underscoring the relevance of optimising these parameters for obtaining the appropriate mechanical characteristics of printed components. These findings show how important raster orientation and printing speed are to the behaviour and durability of 3D-printed components. By determining the optimal mix of these characteristics, manufacturers may develop high-quality, long-lasting components that satisfy their specific demands while lowering manufacturing costs [15].

This study sought to determine how various variables affected the mechanical and physical characteristics of 3D-printed structures. Infill density, infill pattern, infill speed, nozzle temperature, and material type were all taken into consideration. The results showed that 100% infill density components had the greatest Young's modulus, and that as infill density increased,

the strength of the printed components dropped. It was discovered that components printed at an infill speed of 90 mm/s performed the best in terms of tensile modulus. Out of the seven designs studied, the linear infill pattern performed the best in terms of tensile modulus. In terms of tension, bending, and compression, CFR-PLA outperformed the other five materials evaluated. PLA filament prints best around 215 °C. SEM image analysis revealed that the optimum layer arrangement and the least amount of porosity were produced with an infill speed of 90 mm/s. This work emphasises the need of optimising printing parameters to obtain desired features in 3D-printed components by offering useful insights into how different printing settings impact the mechanical and physical properties of 3D-printed products [16].

In this work, the mechanical properties of PLA specimens manufactured with a Rep-Rap Prusa I3 3D printer and the Simplify 3D slicing programme were investigated. The tensile strength of the printed specimens was examined in connection to the process factors using a second-order response surface model. Researchers were able to gain a better understanding of control factors' effects on specimens produced using a Rep-Rap 3D printer thanks to the experimental results. According to the study, strength improves as the number of perimeters rises, while UTS values decline as the infill direction approaches 90 degrees. As the layer thickness gets close to 0.18 mm, the strength values similarly show a clear initial gain before starting to decline. Interesting effects of layer thickness on strain values were observed, with strain values rising at 0.15 mm and falling as the layer thickness reached 0.2 mm. They demonstrated a significantly greater association with UTS and f when the combined effects of the number of perimeters and the direction of the infill were taken into account. By contrasting the anticipated maximum UTS value with the actual value obtained through empirical research for a particular parameter configuration, the statistical model's validity was assessed. These findings suggest that the mechanical characteristics of Rep-Rap 3D printed specimens may be modified by varying the process variables, such as infill orientation, number of perimeters, and layer thickness, presenting enormous promise in a range of applications [17].

The objective of this experiment was to evaluate the strain at break and ultimate tensile strength of the PLA specimens utilising free and open-source 3D printing technology. To do this, the researchers ran a standard tensile test and evaluated the findings. The results of the study demonstrate that the tensile strength of specimens created by open-source 3D printers is

comparable to specimens created by commercial 3D printers. The researchers found that by carefully altering the process factors, the specimens' tensile characteristics could be improved. Because the fibres are parallel to the direction of loading, specimens printed with a 0° raster angle, for example, showed better tensile strength. Additionally, it was discovered that the factors contributing to the printing part's increased strength were the higher raster width and larger bonding area at the lower layer height. It was also shown that the bigger bonding area at the lower layer height and the higher raster width both contributed to the printed part's improved strength. Furthermore, the researchers examined the specimens printed with a 0° raster angle under a microscope and discovered that the fillet region had voids and fibre discontinuities. These problems could be what led to the component failing so quickly. Gaps were also discovered in the cross-section of the printed PLA, a symptom of inadequate diffusion between the layers and rasters and ultimate brittle failure. In conclusion, this work elucidates the different variables affecting the ultimate tensile strength and strain at break of 3D-printed PLA specimens. By carefully modifying the process factors, the researchers were able to increase the strength of the printed pieces. When developing and manufacturing 3D-printed components, voids, fibre discontinuities, and poor diffusion across layers and rasters must be taken into account even if they still have the potential to cause early failure [18].

In order to investigate the effects of infill density on the mechanical properties of 3D-printed PLA specimens, the researchers conducted an experiment utilising FDM. The PLA wire filament used in the experiment has a density of 1.24 g/cm³. In the experiment, the researchers printed specimens with infill densities of 25%, 50%, 75%, and 100% using the optimal printing settings. They found that when the infill density increased from 25% to 100%, the mechanical characteristics of the PLA specimens considerably improved. The materials' hardness, tensile strength, impact strength, and flexural strength were all determined by the investigation. The tensile strength, impact strength, and flexural strength of the PLA specimen with the highest hardness, 97 HRC, were all 53 MPa. The infill density in this PLA specimen was 100%. These results imply that PLA samples printed at 100% infill density might be applied to a range of high mechanical strength applications. It is also important to keep in mind that other factors, such as printing parameters, layer height, and printing speed, can significantly affect the mechanical

properties of 3D-printed objects. More study is needed to completely understand the relationship between infill density and mechanical characteristics in 3D-printed materials [19].

The objective of this study was to determine how temperature impacts the mechanical characteristics of specimens made of 3D-printed PLA. In order to accomplish this, the researchers changed the usual process parameters and looked at the correlations between temperature, printing parameters, and different mechanical properties like tensile stiffness, ultimate tensile strength (UTS), strain, and stress at failure. The researchers used response surfaces to analyse the data and discover the connections between the various parameters in order to obtain these relationships. The findings demonstrated that, in comparison to conventional PLA filaments, the stiffness of 3D-printed PLA filaments decreased from 30% to 16% as the temperature rose from 40°C to 50°C. Tensile tests on the 3D-printed specimens at various temperatures showed that the UTS steadily decreased in all three of the investigated orientations as the temperature rose. The stress at failure, which had a peak value at 30°C and a sharp decline at 40°C, interestingly displayed an anomalous behaviour. Compared to the values seen in the other two orientations, this one was higher. Additionally, between 20 and 30 degrees Celsius, the bonding surface's strength decreased, but the strength of the beads kept the sample's overall force-loading equilibrium stable. The PLA has a glass transition temperature of 40°C, and as the temperature increased, the fragility of the beads caused the stresses to be distributed differently. This led to a magnitude level at the bonding surface that was higher than what was seen at lower temperatures. These results underline how crucial it is to take temperature into account when creating and printing 3D PLA structures. To fully comprehend the underlying mechanisms that underlie the observed variations in mechanical properties with temperature and to optimise the printing process parameters for particular applications, more research is required [20].

The goal of this work was to ascertain if improving the mechanical characteristics of poly(lactic acid) (PLA) samples produced using the rapid manufacturing (RM) process by enhancing the PLA crystallinity by thermal annealing. The inquiry involved 3D printing dumbbell and beam samples at a temperature of 215 °C for mechanical testing. It is widely known that the strength of a semicrystalline material depends on its crystallinity, which is controlled by the intrinsic properties of the polymer and its thermal history. The FDM apparatus and processing parameters

utilised in this investigation led to the discovery that the FDM-PLA exhibited a low degree of crystallinity. To boost the proportion of the ordered phase, the produced samples were heated above the PLA's glass transition temperature. The study's two controlled variables were temperature and time. Lower annealing temperatures required longer annealing periods to achieve the maximum possible crystallinity of roughly 25%. The results of the investigation showed that thermal processing enhanced the samples' strength but did not appreciably alter their modulus. This study has implications for the use of post-processing annealing to improve the longevity of PLA implants produced using an FDM approach. Manufacturers of PLA parts that use thermal prototyping methods should be aware that the post-processing treatment has an impact on the mechanical properties of FDM material, particularly its strength. Thermal annealing strengthens the material by raising its degree of crystallinity [21].

The mechanical characteristics of 3D-printed PLA in various orientations were investigated in a separate research to evaluate its orthotropic behaviour. By adjusting printing parameters including temperature, extrusion speed, and printing head speed, the porosity of the 3D-printed material was reduced. The porosity of the samples utilised in the experiment was around 1%. A 3D-printed material is more sensitive to applied strain rates and has better fracture toughness because it has higher crystallinity and lower ductility than a homogeneous polymer. Due to the material's transversely isotropic elastic response and equivalent axial and transverse stiffness to injection-molded PLA, it has been demonstrated that 3D printing does not influence the material's elasticity. When tested under strain out of plane, the 3D-printed material is more brittle and more ductile when tested in plane. The substance behaves ductile and orthotropically. However, due to the loss of cohesiveness at the start of the tensile response, the compressive flow stress is larger than the tensile flow stress in both directions, suggesting a considerable tension/compression asymmetry. The fracture reaction of the material responds more forcefully axially than transversely. Due to its layered and filamentous structure, which further muddles the microscopic mechanics of fracture, injection-molded PLA is less resilient than 3D-printed PLA. The crystallinity and stiffness of the material are unaffected by an annealing heat treatment with a dwelling temperature slightly below the glass transition temperature, but the strength can be decreased by up to 30%. The work underscores the necessity to modify printing settings to

reduce porosity and improve mechanical qualities and emphasises the orthotropic mechanical properties of 3D-printed PLA [22].

In the study, the performance of PLA tensile specimens produced by 3D printing and compression moulding was examined. The objective was to identify the best manufacturing parameters by using experiment design to investigate the impact of processing factors on the tensile properties of compression-molded specimens. The results show that by employing the optimal 3D printing process settings, specimens may be produced that have tensile properties that are comparable to those produced by using traditional manufacturing methods. The moisture absorption of PLA specimens produced by compression moulding and 3D printing was evaluated. 3D printed specimens were shown to absorb much more water than conventionally manufactured specimens (3.92% vs. 0.83% on average), which reduced their tensile strength and modulus by 28.4% and 7.2%, respectively. Tensile strength of compression-molded specimens reduced by 12.0% while tensile modulus increased by 14.1%. Because voids made it easier for moisture to infiltrate into 3D printed specimens, their mechanical performance was reduced [23].

The compressive strength of samples made from 3D-printed PLA and a number of surface profile characteristics were examined. The results demonstrate that increasing infill density enhances the compressive strength of PLA specimens printed using 3D printing technology. With a value of 121.35 MPa, the Hilbert curve pattern exceeded preceding designs in terms of compressive strength. Rectangular, line, honeycomb, archimedean, and octagram spiral patterns came in second and third, respectively, with values of 78.88 MPa, 73.84 MPa, and 60.01 MPa. The surface smoothness of the specimens greatly enhanced for rectilinear and Hilbert curve patterns; however, for line patterns, it deteriorated as the infill density fell (R_a rose from 1.994 at 80% to 2.508 at 20%). When the infill density was dropped from 80% to 20%, the roughness value (R_a) fell for the Hilbert curve (53.66%) and rectilinear (39.84%) patterns but rose for the line pattern (25.77%). Given that it had the lowest surface roughness value at a 20% infill density ($R_a = 1.14 \text{ } \mu\text{m}$) in comparison to the Hilbert curve and line patterns ($R_a = 2.185 \text{ } \mu\text{m}$ and $2.508 \text{ } \mu\text{m}$, respectively), the rectilinear pattern is the best pattern in terms of surface roughness quality. In terms of surface roughness, Hilbert curves and lines outperformed rectilinear patterns at 80% infill density ($R_a = 1.895 \text{ } \mu\text{m}$ vs. $4.716 \text{ } \mu\text{m}$ and $1.994 \text{ } \mu\text{m}$, respectively). It was found that the Hilbert curve pattern had the optimum compressive strength for surface applications [24].

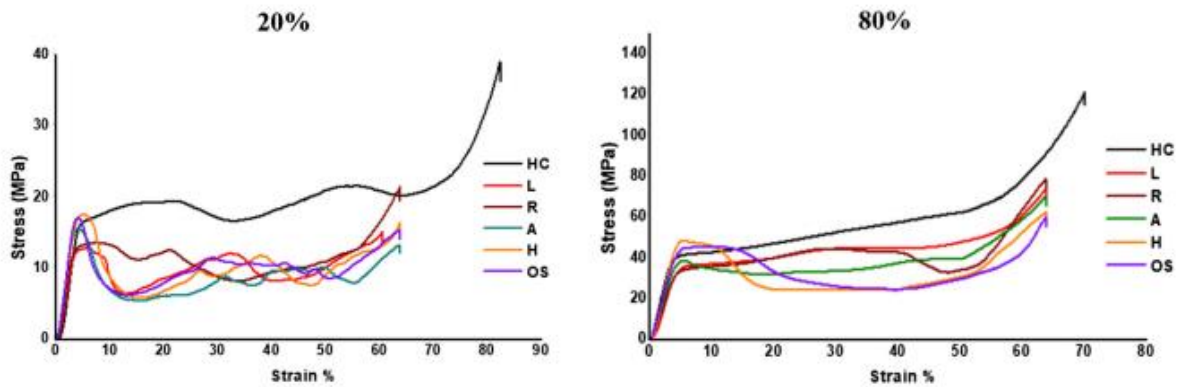


Figure 6: Comparison of compression strength for 20 and 80% infill density [24]

The purpose of this study is to look at how different FDM process settings affect the mechanical properties of 3D-printed objects. In particular, the experiment examines the effects of layer height, building direction, and infill % on the tensile property of the printed pieces. According to the findings, all three factors have an impact on the components' tensile strength, with infill % and layer height having a more pronounced effect at higher levels. The research pinpoints the perfect combination of manufacturing factors for creating 3D-printed things with the greatest tensile strength. According to TOPSIS research, the optimum process factors for producing the maximum tensile strength are 80% infill, 0.2 mm layer height, and X building orientation. Furthermore, the research finds that Y building orientation, 0.2 mm layer height, and 80% infill are the optimal process variables for attaining the maximum compressive strength, which is consistent with the experimental findings [25].

Understanding how manufacturing procedures affect a part's tensile and flexural strength is the main objective of this study. As FDM process parameters, the study considers the infill geometry, layer thickness, and number of perimeters. The samples' tensile strength and flexural strength were determined in accordance with ASTM D638 IV and ASTM D790, respectively. L9 Taguchi orthogonal array and the ANOVA technique were employed in the study to examine how process factors affected these features. The findings showed that a layer thickness of 0.100 mm, 6 perimeters, and gyroid infill geometry are the crucial variables for an ideal tensile strength of 44.925 MPa. The stiffness and tensile strength increase as the number of perimeters increases. The ideal layer thickness for flexural strength is 0.150 mm, with four perimeters and a concentric infill geometry, resulting in an expected strength of 115.344 MPa. Flexural strength is enhanced

by a narrower air gap that is made possible by raising the layer height. The principal effect diagram, interaction plot, and optimal factor algorithm were used to establish the right values for the tensile and flexural strengths [26].

This study's goal was to investigate how the FDM process settings affected the mechanical characteristics of 3D printed samples. Tensile tests were carried out using UTM to assess how layer thickness and cooling rate affected the tensile strength in both horizontal and vertical orientations. According to the study, the tensile strength rose for the horizontal orientation from 0.05 to 0.1 mm of layer thickness but declined for layers thicker than 0.2 mm. The tensile strength, however, was little impacted by the cooling rate. The sample with the best tensile strength had a layer thickness of 0.2 mm for the vertical orientation, however the strength fell as the layer thickness grew. In the case of vertical orientation, cooling rate had a more apparent impact on the tensile strength, with quicker cooling resulting in much lower tensile strength. Additionally, the build time was significantly impacted by the cooling rate, with thicker layers printing more quickly. As a result, it may be said that layer thickness and printing time have an inverse relationship. In contrast to higher layer thickness values, which produced quicker prints with lower tensile strength, lower layer thickness values produced slower prints with better tensile strength [27].

The purpose of this study is to look at the connection between infill density and infill patterns. Printing PLA samples for the study involves using three infill densities—25%, 50%, and 75%—as well as three infill patterns—grid, trihexagonal, and concentric. A print speed of 50 mm/sec, a print temperature of 210 °C, and a build bed temperature of 70 °C are used to create the samples. The samples are subsequently put through tensile testing utilising a UTM machine at a strain rate of 5mm/min in compliance with ASTM 638D standards.

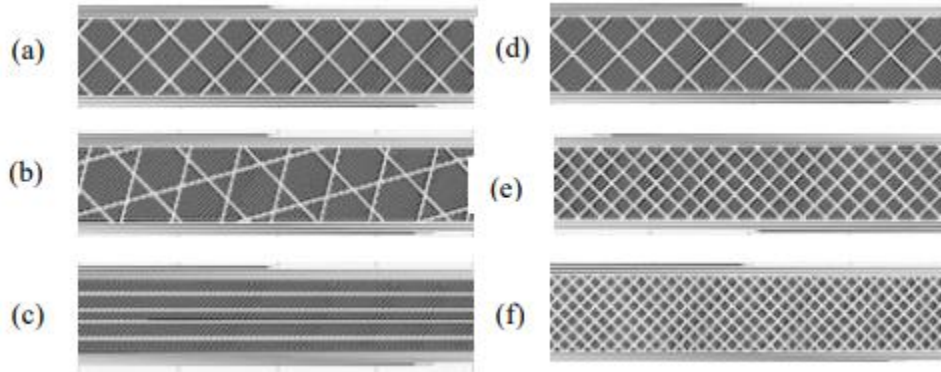


Figure 7: Infill patterns: (a) grid, (b) tri-hexagonal, and (c) concentric. Grid pattern infill densities: (d) 25%, (e) 50%, and (f) 75%. [28]

The results show that for both the grid and triangle infill designs, the ultimate strength rises with infill density. At 25% density, the maximum strengths for the grid and tri-hexagon patterns are 29.7 MPa and 27.8 MPa, respectively, while at 50% density, they are 31.5 MPa and 30.6 MPa. At 75% density, the ultimate strength is calculated to be 35.4 MPa for the grid design and 37.3 MPa for the triangular pattern, respectively. This tendency is not present, though, when the infill pattern is concentric. The final strengths for the concentric pattern are 32.6 MPa, 44.3 MPa, and 42.2 MPa for infill densities of 25%, 50%, and 75%, respectively. The infill pattern with concentric spheres has the maximum tensile strength. Additionally, the grid design with 100% infill density is indicated to have a yield strength of 48.2MPa. However, it is shown that at 100% infill density, infill patterns minimally affect mechanical qualities [28].

Another study examines the impact of pattern and infill density on the tensile strength of PLA. By changing the infill density from 10% to 90%, nine examples of each of the 13 distinct infill patterns are produced. The ISO 572-2-compliant dog-bone type sample is produced, and it is printed on a flatbed with a layer height of 0.15mm, a raster angle of 45°, and a printing temperature of 205°C. There are 130 examples in all, printed with different infill densities and patterns. Tensile testing is done using a Shimadzu AGS-X UTM with a 1mm/min strain rate. The results demonstrate that the circular infill design provides the greatest outcomes at a 90% infill rate. As infill density rises from 10% to 90%, tensile strength for circular infill patterns improves by 96%. From 18.2 MPa at 10% density, the tensile strength rises to 90% infill density. By increasing infill density by up to 60%, zigzag infill patterns' tensile strength can be enhanced. As

infill density is raised, tensile strength drastically declines. The maximum tensile strength is calculated to be 25.1MPa at a 60% infill density. The tensile strength decreased to 20.9 MPa at 90% infill density. The improvement in ultimate tensile strength for cross-infill patterns as infill density changes from 10% to 90% is just 7%. With a tensile strength of 18.7 MPa at a 90% infill density, the PLA specimen created by the cross infill pattern is also the weakest. The octet infill pattern, the weakest specimen, has a tensile strength of 15.2 MPa at a 10% infill density and increases to 77% at increasing infill densities. Tensile strength for a PLA specimen with an octet infill pattern is 26.4 MPa at 90% infill density [29].

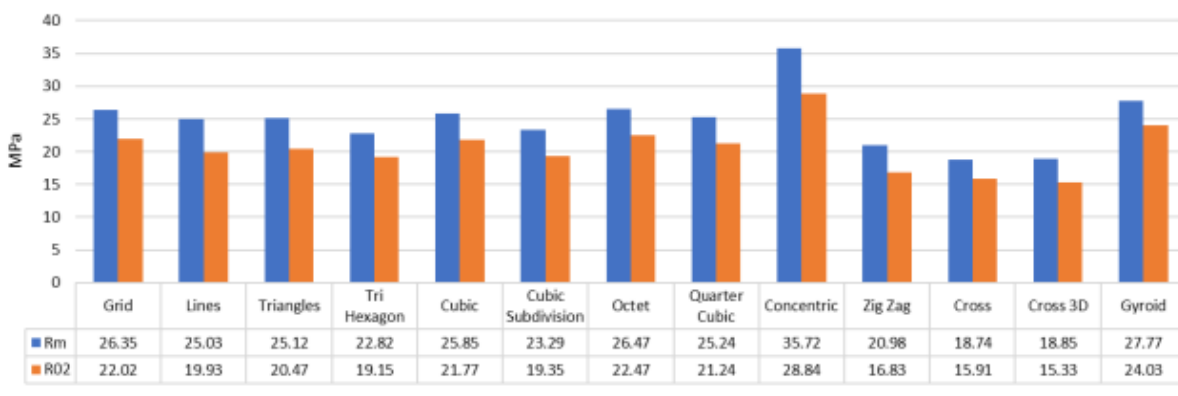


Figure 8: Maximum ultimate tensile strength (RM) and yield strength (R02) for every infill pattern [29]

The goal of this study is to evaluate the mechanical characteristics of PLA and determine how various printing conditions impact them. The study focuses on how the mechanical characteristics of PLA samples are impacted by layer thickness, build orientation, and feed rate. Layer thicknesses of 0.06, 0.12, 0.18, and 0.24 as well as feed rates of 20, 50, and 80mm/sec are taken into account. Additionally, three alternate construction orientations—flat, on-edge, and upright—are utilised. The raster angle is held constant at 0° and the printing temperature is maintained at 210°C. The PLA samples are prepared in accordance with ASTM 638D and 790D standards for tensile and flexural testing specimens, respectively [30].

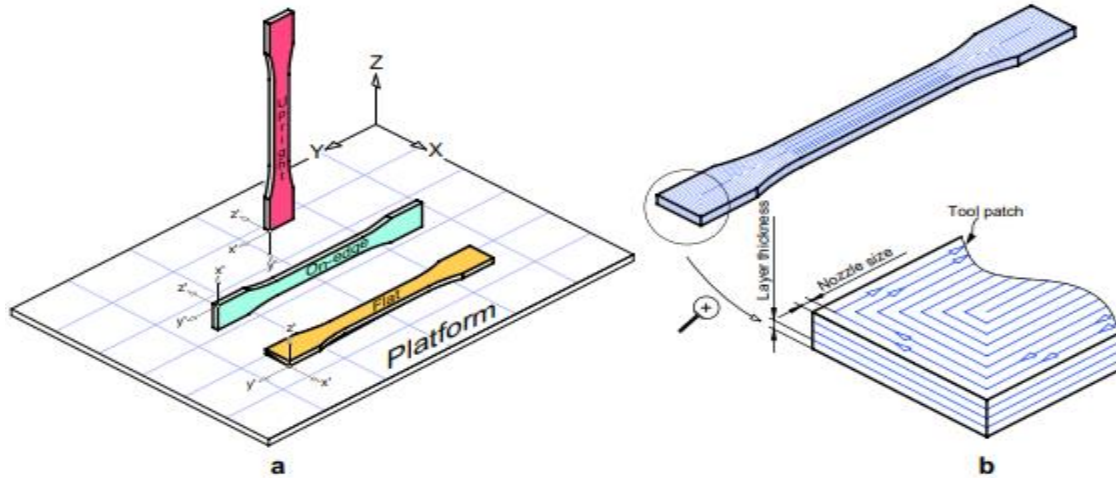


Figure 9: Process parameters: a) Build orientation. b) Layer thickness [30]

The findings of this study demonstrate that the fabrication process's printing settings significantly affect the mechanical characteristics of PLA samples. Particularly, the orientation of the structure plays a crucial role in establishing the samples' mechanical characteristics. While the on-edge orientation results in the highest flexural and tensile strength, the inner layer fails in an upright orientation, indicating a weaker link between the layers in the sample. The mechanical properties of PLA samples are significantly influenced by the layer thickness. It was discovered that the upright orientation samples show an increase in tensile and flexural strength as layer thickness increases. The improvement in strength is negligible for layer thicknesses between 0.12 and 0.24 mm for flat, on-edge constructed samples. The feed rate applied during printing is another important element that has an impact on the samples' mechanical characteristics. The results show that for upright-built samples, increasing feed rate results in a reduction in tensile and flexural strength. For flat and on-edge oriented samples, however, the impact of feed rate on these mechanical characteristics is minimal. This study clarifies the relationship between several printing parameters, including build orientation, layer thickness, and feed rate, and the mechanical properties of PLA samples. The findings indicate that the optimal printing circumstances, such as on-edge orientation and a certain layer thickness, should be taken into consideration in order to produce the necessary mechanical characteristics in PLA samples [30].

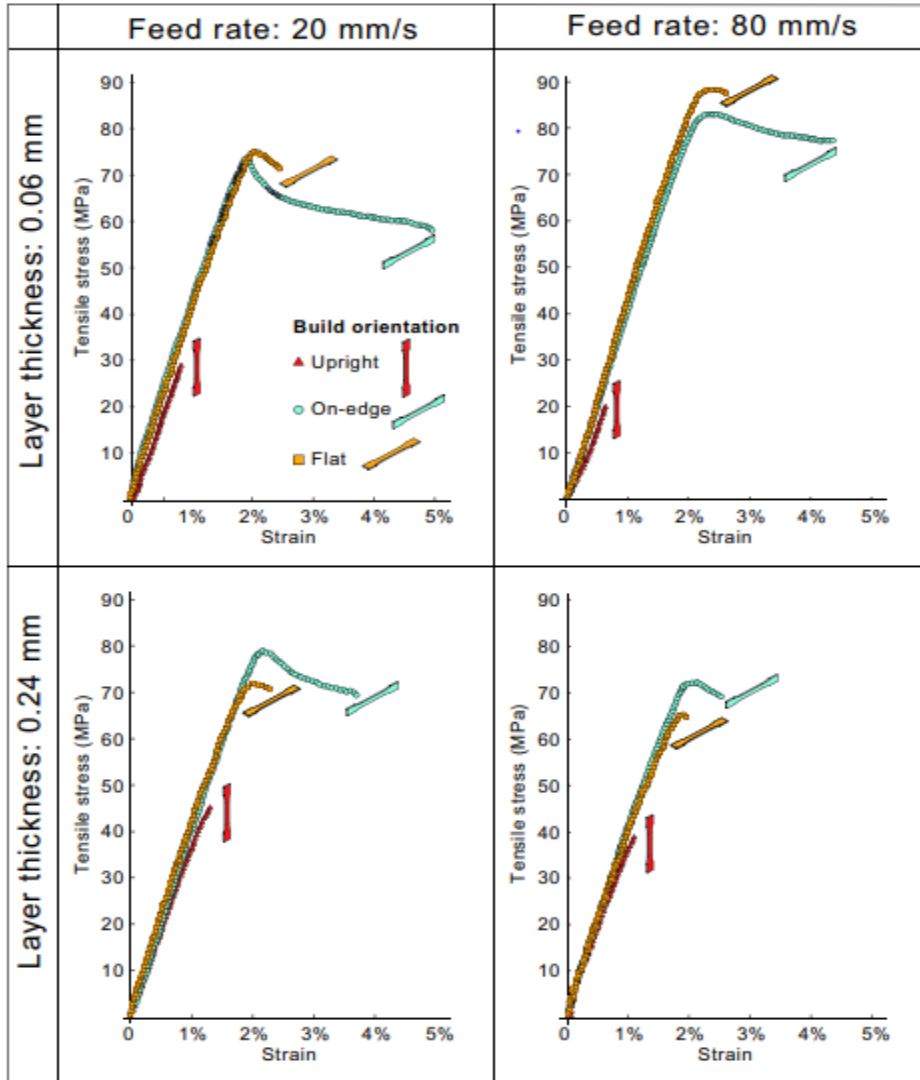


Figure 10: Average stress-strain curves for the tensile specimens under different printing conditions [30]

The tensile characteristics of PLA specimens created using various 3D printing settings were examined in a separate investigation. The specimens were made in compliance with ASTM 638D standards and utilised three various infill patterns—diamond, linear, and hexagonal—at three different infill densities. Maker-Bot Maker Ware was used as the slicing programme, with a printing temperature of 210°C, a bed temperature of 60°C, and a layer thickness of 0.20mm. The mechanical testing instrument tested the samples for tensile strength using a 3kN load cell while maintaining a constant cross-head speed of 3mm/min. Infill density directly correlated with an increase in tensile strength. With tensile strengths of 31.40 MPa and 42.67 MPa, respectively, and linear infill patterns at infill densities of 25% and 75%, the best results were obtained. The

diamond pattern's greatest tensile strength was found to be 35.56 MPa at a 50% infill density [31].

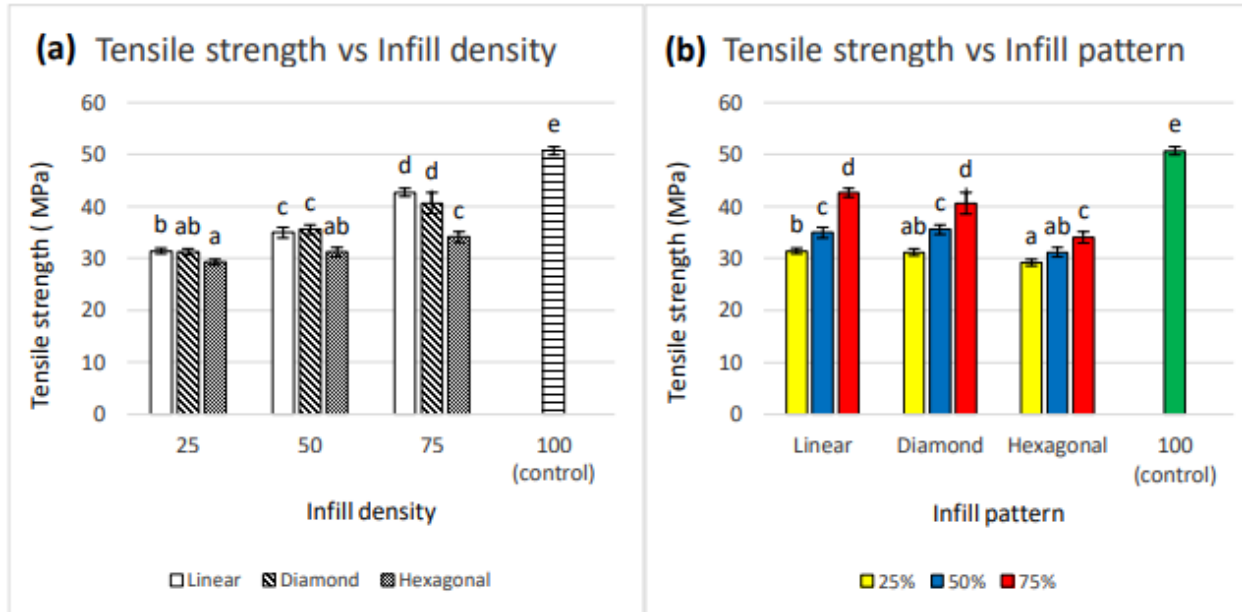


Figure 11: Effects of infill pattern and infill density on the tensile strength of the 3D-printed specimens, (a) tensile strength vs. infill density and (b) tensile strength vs. infill pattern [31]

An investigation was made into the possibility of enhancing interlayer tensile strength by post-processing of extruded samples. The study examined mechanically strengthened semi-crystalline PLA and amorphous PETG annealed samples. It was thought that short carbon fibres decreased the tensile strength between layers. Clean PLA and PETG samples as well as carbon-reinforced CFR-PLA and CFR-PETG samples were produced for the investigation using a 3D printer. The ASTM 638D type 1 specimens were produced. With a bed temperature of 90°C and an extrusion temperature of 250°C, PETG was produced. PLA was extruded at a temperature of 210°C, whereas the bed temperature was 55°C. The study found that PETG with carbon fibre reinforcement had considerably lower interlayer tensile strength. Unannealed PETG CF specimens were found to have a mean interlayer tensile strength of 12.4 MPa. The interlayer tensile strength of PETG-CF samples was somewhat increased, reaching 13.8 MPa after being annealed for 30 minutes at a temperature higher than the glass transition temperature. The interlayer tensile strength of the specimens increased to 24.4 MPa and 32.4 MPa, respectively, after further annealing for 240 minutes and 480 minutes. The interlayer tensile strength of clean PLA specimens that were 3D printed was 32.3 MPa, and annealing the PLA specimens at 120°C

had no effect on this tensile strength. The PLA specimens' tensile strengths somewhat increased after being annealed at 90°C for 30, 240, and 480 minutes. The interlayer tensile strength of the PLA specimens decreased as a result of the addition of carbon fibre. Unannealed and annealed PLA-CF specimens were tested at 120°C for 30, 240, and 480 minutes to determine their relative interlayer tensile strengths. These values were 16.0 MPa, 16.5 MPa, 16.9 MPa, and 16.8 MPa. The interlayer tensile strengths of the samples increased to 16.8, 30.8, and 29.9 MPa, respectively, after being annealed at 90°C for 30, 240, and 480 minutes. The interlayer tensile strength of the CF-PLA specimens did not significantly change after annealing at 120°C, however it did significantly increase after 240 and 480 minutes at 90°C [32].

This study's major goal is to determine how in-plane raster orientation affects the fracture and tensile strengths of poly-lactic acid (PLA) samples made using the fused deposition modelling technique. To examine the mode I fracture and tensile behaviour of 3D-printed PLAs, four different raster angles of 0/90°, 15/75°, 30/60°, and 45/45° were chosen for dog-bone and semi-circular bending (SCB) specimens. The SANTAM STM-150 universal testing machine was utilised for the tensile tests, which were carried out under displacement control at a speed of 0.5 mm/min. Each tensile sample's deformation was detected using the digital image correlation (DIC) approach. An optical method called DIC employs digital pictures to calculate the stresses and full-field displacements of the damaged object. It was discovered that the raster orientation had an impact on the fracture stress, with specimens with 45/45° and 0/90° angles having the strongest and lowest fracture resistance, respectively. The most anisotropic feature in the elastic area was the elastic modulus, which among the several raster orientations had the maximum anisotropy of 19%. The material showed a more anisotropic behaviour in terms of its elongation at break, with the biggest and smallest values being obtained at raster angles of 45/45° and 0/90°, respectively [33].

A subsequent research project will examine how different 3D printing settings affect the tensile strength and hardness of PLA material. The FDM technique will be used to the testing specimens with various build orientations, raster direction angles, and layer heights. To create the tensile test samples, the filament will be manufactured using a 0.4 mm nozzle and different printing parameters. The construction platform and printing platform will be heated to 195 °C and 60 °C,

respectively, for the printing process. The 3D printing model (STL file) will be sliced using Ultimaker Cura 4.3, and the same programme will also be used to control the 3D printing parameters. The output of the file (G-code) appropriate for the manufacturing machine follows. The tensile test specimens will be printed in accordance with ISO 527-2 type 1B. The primary goal of the study is to determine how white PLA's tensile strength is affected by layer thickness, print orientation, and raster direction angle. The on-edge sample, which measures 1.896 0.044 GPa and 49.12 0.78 MPa, is anticipated to have the greatest Young's modulus and ultimate tensile strength values of all the specimens examined. This is because the inter-layer fibres and roadways are bonded together, increasing the overall strength of complex structures. Additionally, the samples' surfaces will have shells (contours) that are tightly bonded and parallel to the direction of the testing force, increasing their strength. Due to its robust structure, flat print orientation will have the best elongation at UTS and elongation at break, while on-edge print orientation is projected to have the greatest Young's modulus, UTS, and hardness [34].

In accordance with ISO/ASTM 52900, the current study focuses on the application of fused deposition modelling in material extrusion additive manufacturing to produce components with the best possible mechanical qualities. Dogbone-shaped tensile samples were created using a 3D printing programme with five different filling patterns and four different nozzle temperatures in order to examine the effects of printing and annealing conditions on the physical and mechanical characteristics of PLA-based components. The printed samples were then repeatedly annealed at each of three distinct temperatures. Rheometrical measurements were used to assess the samples' mechanical characteristics, and modifications to those qualities were looked at. To examine the impact of extrusion temperature on the mechanical properties of PLA-printed objects, four samples were printed at various nozzle temperatures. Although the strain at break value rises from 34 to 56 MPa with increasing nozzle temperature, it seems that nozzle temperature has no effect on strain at break. Although heat annealing typically improves the mechanical characteristics of polymeric materials, PLA-based samples showed negative effects because of the potential for stress buildup. The findings imply that heat annealing of PLA-based 3D-printed items ought to be avoided. Additionally, it was discovered that the mechanical properties of the finished product are greatly influenced by the way the extrusion head moves [35].

The goal of this study is to investigate the physical alterations brought about by PLA 3D printing, with a particular emphasis on how porosity, crystallinity, and mechanical characteristics of the printed objects interact. Investigated is the effect of build-platform temperature. An industrial 3D printer with a set nozzle temperature of 180°C, a layer height of 0.1 mm, and a raster angle of 45° is used to carry out the 3D printing. Injection moulded samples and square specimens printed with different thicknesses using PLA filaments are both created for comparison. In the middle and upper layers of the printed specimens, many pores have formed, according to cross-sectional examination. A higher degree of orientation and lower build-platform temperatures result in thinner samples and better mechanical characteristics. The mechanical qualities of the printed samples, however, are inferior to those of the injection-molded examples. The internal tensions and crystallinity of the printed samples are being changed by annealing them for 10 minutes at 120 degrees Celsius as a solution to this problem. After the heat treatment, the outcomes demonstrate an improvement in storage modulus as measured by DMA [36].

The focus of this research is on optimizing the tensile creep behavior of 3D printed objects that use polylactic acid (PLA) material with the Fused Deposition Modeling (FDM) technique. The design of the creep test specimens is in accordance with the requirements for geometry (D2990) outlined by ASTM. To achieve this goal, a MakerBot desktop 3D printer, which is open-source, is used for the 3D printing process. The Response Surface Methodology (RSM) is employed to predict the creep rate and rupture. The process input variables that are examined include layer height, infill percentage, and infill design, which include linear, hexagonal, and diamond designs.

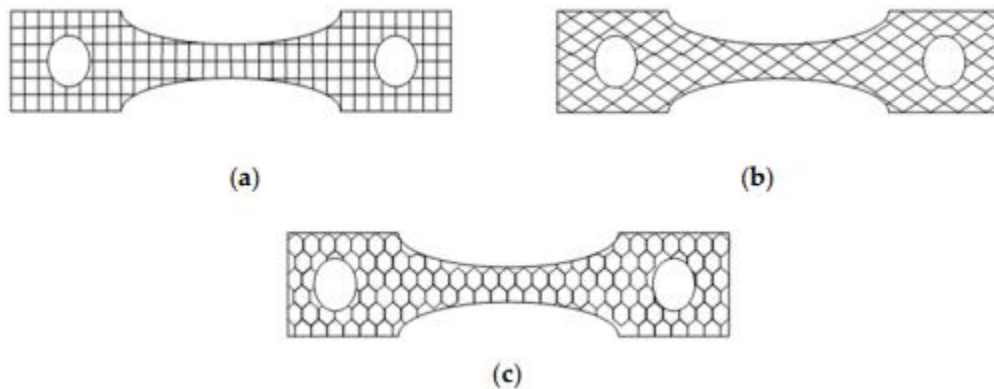


Figure 12: The adopted infill patterns: (a) linear, (b) diamond, (c) hexagonal. [37]

The objective of this work was to improve the tensile creep behaviour of FDM-printed PLA items. The creep test specimens were designed in accordance with ASTM standard geometry specifications and printed on a desktop MakerBot 3D printer. It was done by using Response Surface Methodology (RSM) to forecast creep rate and rupture. The analysis of variance (ANOVA) results showed that layer height, infill%, and infill patterns had the most significant effects on creep rate, while infill pattern had the greatest impact on rupture time. The categorical central composite design was used to schedule 39 experimental runs. The 0.1 mm layer height and 100% infill percentage for the hexagonal pattern were determined to be the ideal settings for both responses. When layer height was increased from a low level to a medium level, the creep rate for linear designs increased; however, when layer height was increased from a medium level to a high level, it reduced. The creep rate reduced as the infill% rose from a low to a high level. However, for hexagonal layouts, the creep rate only slightly dropped from a low to a high infill% but rose with layer height. Similar outcomes for the creep rate were also seen for the diamond design. raising the infill% from a low to a high level decreased the rupture time of linear designs, although marginally raising the layer height had the opposite effect. Because it strengthened the bond between layers and improved mechanical performance, lower layer height gave good mechanical strength. Similar to how material density rose, mechanical strength did as well. Six of the hexagon's sides had stronger bonds, which increased the structure's tensile strength since those molecules were in close proximity to it. The distance between printed layers widened and the bonding strength decreased when the infill % was decreased [37].

Infill density, printing speed, and layer thickness were the three primary process factors that were the subject of this study's investigation into the tensile characteristics of PLA samples. The Taguchi design of experiments approach was used to maximise the parameters while minimising the number of trials in order to attain the best mechanical characteristics, lightweight, and speed of printing. In order to get the required results, the Taguchi technique also used the Analysis of Variance (ANOVA) method or Signal to Noise (S/N) ratio. By examining the variance between many groups, the ANOVA approach was used to evaluate the overall influence of each manufacturing process parameter on the final attributes. The findings were evaluated by modifying the process parameters based on the average output response, while the S/N ratio

approach was used to estimate the response change to the nominal value in various noise circumstances.

Test number	Printing Speed (mm/sec)	Layer thickness (mm)	Infill density (%)
1	20	0.1	20
2	40	0.2	20
3	20	0.1	40
4	40	0.2	40
5	20	0.2	60
6	40	0.1	60
7	20	0.2	80
8	40	0.1	80

Table 1: Process parameters for sample preparation[38]

A quasi-static tensile test was conducted on each specimen made using FDM 3D printing at room temperature and with a loading rate of 1 mm/min in order to assess the mechanical characteristics of PLA specimens. The infill density, printing speed, and layer thickness process parameters were changed to see how they affected the specimens' mechanical characteristics. The outcomes showed that the specimens printed with an infill density of 80%, a printing speed of 40 mm/s, and a layer thickness of 0.1 mm had the highest ultimate tensile strength and elastic modulus. However, the ideal process parameters were discovered to be an infill density of 80%, a printing speed of 40 mm/s, and a layer thickness of 0.2 mm for obtaining the maximum failure

strain during printing. These results show the substantial influence of process variables on the mechanical characteristics of PLA specimens and may be exploited to raise the calibre of 3D printed goods. To investigate how various process factors affect the mechanical characteristics of other materials, more research may be done [38].

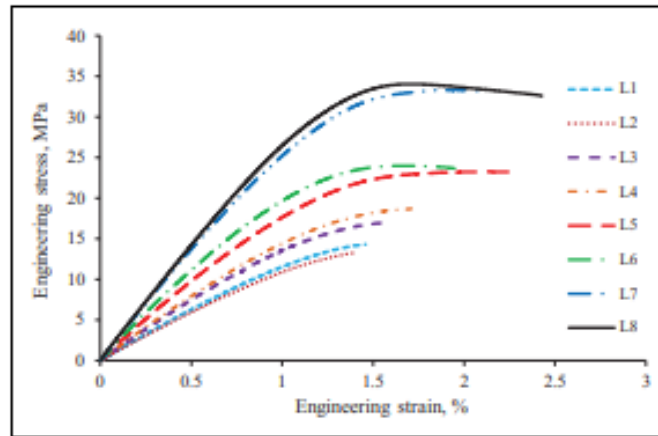


Figure 13: The stress–strain curves of eight experiments designed by the Taguchi method. [38]

To find out how different 3D printing settings affected the mechanical properties of PLA specimens, a test was run. A 3D printer with a nozzle diameter of 0.4 mm and a layer height of 0.2 mm was used in the experiment. A number of variables, including printing speed, temperature, and infill %, were taken into account while analysing the 3D printing parameters. The PLA specimens underwent evaluations for tensile strength, elastic modulus, and elongation at break. The results showed that altering printing speed had an immediate impact on tensile strength and elastic modulus, with an increase in these parameters shown as printing speed was raised. On the other hand, when the temperature rose, both the aforementioned characteristics and elongation at break decreased. However, elongation at break reduced while tensile strength and elastic modulus improved with an increase in infill %. The findings of the study demonstrate the importance of 3D printing settings on the mechanical characteristics of PLA specimens. These results may be used to improve the quality of 3D printed objects and can also be the starting point for more investigation into how different 3D printing parameters affect PLA and other materials [39].

The impact of environmental factors on the mechanical characteristics of components made using open-source 3D printers is discussed in this article. Under realistic environmental circumstances, the authors conducted tests to evaluate the mechanical characteristics of parts manufactured of ABS, PLA, and PETG filaments. The results showed that the environment's temperature and humidity had a significant influence on the mechanical characteristics of the components. The authors came to the conclusion that while 3D printing has promise for creating components with adequate mechanical qualities, maintaining the appropriate performance necessitates exact environmental monitoring and management. The article gives a thorough summary of the status of 3D printing technology today, its possible benefits and drawbacks, and how the environment may alter a component's mechanical qualities. The authors also provided a thorough explanation of the experimental approach taken as well as the outcomes. This article offers insightful information on the subject of 3D printing and its prospective uses in the industrial industry. Given that they can considerably affect a component's performance, environmental factors and how they affect mechanical qualities of 3D printed components must be taken into account. In conclusion, the authors have significantly advanced the subject of 3D printing by offering a complete analysis of its present status, the impact of environmental factors on component mechanical qualities, and the possibility for its application in manufacturing [40].

This study investigates how the mechanical and water absorption properties of composite materials consisting of 3D-printed wood and PLA are affected by the printing layer thickness. A 3D printer with a build volume of 20 cm x 20 cm x 20 cm was utilised for the investigation. The wood/PLA composite material was made using wood flour and polylactic acid (PLA) at a weight ratio of 50:50. Tests on the specimens' mechanical and water absorption capabilities revealed that the printing layer thickness varied from 0.1 to 0.6 mm. The findings demonstrated that the wood/PLA composite materials' capacity to absorb water increased together with the thickness of the printing layer. The enhanced water absorption was assumed to be caused by the specimens' greater porosity, which came about as a result of the thicker layers. The mechanical properties of the specimens also improved as the printing layer thickness increased. The better adhesion between layers and the thicker layers' higher density were connected to their higher mechanical properties. Based on the results, it was concluded that the mechanical properties and water absorption of 3D-printed wood/PLA composite materials are greatly influenced by the thickness

of the printing layer. These results may enable the 3D printing process to generate wood/PLA composite materials with the desired properties [41].

The goal of this critical analysis of the literature is to assess the present level of knowledge about the production of PLA parts using FDM 3D printing technology. Previous research has shown that FDM 3D printing can create PLA items with great surface quality and dimensional precision. The technique is still challenged by the components' strength and post-processing, though. Recent research have recommended adding fillers like carbon fibre and graphene to PLA parts printed using FDM to increase their mechanical qualities in order to address the issue of strength. It has been demonstrated that using these fillers makes the components stronger without sacrificing their dimensional precision and surface quality. This strategy is especially useful for applications that call for high-strength PLA components. To enhance the surface quality of PLA components, post-processing techniques such as heat treatment and surface finishing have also been researched. These techniques have been demonstrated to make components less rough and more aesthetically pleasing. Further research is still needed to determine how post-processing affects the components' mechanical characteristics. In general, FDM 3D printing is a practical way to create PLA parts. To completely optimise the technology, it is evident that there are still certain issues that must be resolved. In order to do this, further study is required to examine how fillers and post-processing methods might be used to increase the strength and surface quality of PLA components. In order to maximise the potential of the technology, new uses of FDM 3D printing in the production of PLA parts need to be researched [42].

This study investigates the mechanical characteristics of 3D-printed components. The researchers used several 3D printing processes, including FDM and Selective Laser Sintering (SLS), to test a range of materials, including ABS, PLA, and PCL. Tensile, flexural, and impact strength tests were performed on the parts. The outcomes demonstrated that the 3D-printed components' mechanical qualities were equivalent to those of their injection-molded counterparts. The 3D-printed parts' tensile strength, flexural strength, and impact strength, which were all higher than the impact strength of injection-molded parts, ranged from 25 to 64 MPa, 10 to 50 MPa, and 10 to 20 J/m, respectively. The study came to the conclusion that a variety of applications needing mechanical strength may make use of 3D-printed components. The

components may also be used in severe situations since they showed strong mechanical characteristics even at low temperatures. The study also covered the drawbacks of 3D printing technology, such as the scarcity of materials and the lack of precision in manufactured items. The scientists advocated for more study to enhance the mechanical characteristics of 3D-printed components, widen the selection of materials that may be used, and boost the precision of printed parts. In conclusion, this study offers insightful information about the mechanical characteristics of 3D-printed components. It proves that 3D printing technology can create parts with mechanical qualities similar to those created by conventional injection moulding. However, further study is required to enhance the mechanical characteristics of 3D-printed components and broaden the scope of uses for them [43].

The impacts of nozzle diameter on the surface quality, mechanical strength, thermal stability, printing speed, and dimensional accuracy of 3D-printed goods using a Prusa i3 Mk3s printer were examined in a research by Czyzewski et al. (2020). According to the study, increasing the nozzle diameter led to improvements in dimensional accuracy, surface quality, mechanical strength, and thermal stability as well as a reduction in printing time. This is in line with related research from the area, including Li et al. (2018) and Jang et al. (2019), which discovered that a bigger nozzle diameter enhances the mechanical qualities and surface quality of 3D-printed items. These research shed important light on how the nozzle width affects the functional qualities of 3D-printed items. It is possible to enhance the functionality of 3D-printed objects and create fresh and creative uses for the technology by customising the nozzle diameter. In order to acquire the greatest potential functional qualities for 3D-printed items, more study is required to optimise nozzle diameter and other printing parameters [44].

This study focuses on how layer thickness affects the flexural characteristics of specimens made of 3D-printed polylactic acid (PLA). The flexural properties of the polymers used in 3D printing, which are a fundamental aspect of these materials, can be considerably impacted by the thickness of the printed layers. After printing the PLA samples at three different layer thicknesses (0.2 mm, 0.3 mm, and 0.4 mm), the researchers measured their flexural strength, flexural strain, and flexural stress. The results showed that increasing layer thickness decreased the flexural modulus, flexural strength, flexural strain, and flexural stress of the PLA samples. This research

provides informative data on the relationship between layer thickness and the flexural properties of 3D-printed PLA samples, which will assist designers and producers in producing 3D-printed PLA components with improved flexural properties. The findings might potentially be used to develop accurate projection models for the flexural properties of 3D-printed PLA samples and to optimize the flexural properties of 3D-printed PLA components by adjusting layer thickness [45].

The study by Vinoth Babu et al. (2020) examines the effects of slicing parameters on the mechanical characteristics and surface quality of 3D-printed CF/PLA composites produced using the FDM method. To examine the connection between these factors and the characteristics of the composites, the authors ran tests. The outcomes demonstrated that layer height, followed by slice thickness and print speed, had the greatest impact on the composites' mechanical characteristics and surface quality. Surface roughness decreased with increasing layer height, slice thickness, and print speed. It also decreased with increasing layer height alone. Additionally, the stiffness and strength of the composites tended to improve as layer height, slice thickness, and print speed were increased. Overall, this work contributes valuable knowledge on the effects of slicing parameters on the characteristics of 3D-printed CF/PLA composites. The results may be applied to enhance the slicing parameters, enhance the quality, and enhance the functionality of composites produced by 3D printing [46].

This study report compares and contrasts the mechanical characteristics of PLA items made using FDM printing both before and after heat treatment. This study's goal is to find out how thermal treatment, a frequently used, easily accessible, and reasonably priced substance, influences the mechanical characteristics of FDM printed objects manufactured from PLA. Tensile and flexural tests were used to assess the mechanical characteristics. The findings showed that the PLA components' tensile strength and modulus, as well as their flexural strength and modulus, had been significantly improved by heat treatment. This suggests that applying heat treatment to FDM produced items can significantly improve their mechanical qualities. In conclusion, this study offers crucial understandings into how thermal treatment affects the mechanical characteristics of PLA-based FDM printed objects. For applications like fast prototyping, where mechanical characteristics are crucial, the study's findings may be helpful.

Additionally, this study offers a practical method for improving the mechanical qualities of FDM printed items. Consequently, this study makes a substantial contribution to the field of fast prototyping [47].

CHAPTER 2: METHODOLOGY

2.1 Material:

The thermoplastic polymer PLA, which can be purchased commercially and is made from renewable resources such as maize starch, sugarcane, or cassava, is the substance used in this study. A versatile material, PLA is used in a number of products and processes, such as 3D printing, consumer goods, and packaging. One of PLA's biggest benefits is that it is environmentally friendly because it is compostable and biodegradable, which makes it a great alternative to other kinds of plastic. PLA is useful for a wide range of applications since it is also reasonably simple to make and has high dimensional stability. The physical and mechanical characteristics of PLA can vary depending on the particular polymer used. These characteristics can range from an amorphous, glassy polymer to a semi- or highly crystalline polymer with a glass transition temperature of 60–65 °C, a melting temperature of 130–180 °C, and a tensile modulus of 2.7–16 GPa. In addition, PLA is soluble in a variety of solvents, such as heated benzene, dioxane, and tetrahydrofuran.

The major objective of this work is to employ the fused deposition modelling approach to evaluate how the printing settings, both with and without annealing, impact the mechanical properties of 3D-printed PLA samples. While certain variables are kept constant, others are changed to see how they affect the tensile strength of the samples.

2.2 Selection of Parameters and Levels

Infill density, Layer thickness, Infill pattern, Infill temperature, and annealing temperature are the parameters selected at different levels for the study. Table 1 shows the level and values of these parameters. Printing speed and bed temperature are kept constant for each sample. Default values of the number of inner and outer layers and thickness are used by Ultimaker Cura.

Parameters	Level 1	Level 2	Level 3
Layer Thickness	0.16	0.20	-
Infill density	70	80	90
Infill patterns	Octet	Tri-hexagonal	Gyriod
Infill temperature	195°C	205°C	215°C
Heat treatment temperature	0°C	90°C	130°C

Table 2: Values of process parameters

Printing speed and bed temperature are constant parameters. The printing speed for each sample is 50 mm/sec, and the bed temperature is 50°C. All samples are prepared with flat orientation on a 3D printer.

Parameters	Level	Unit
Printing Speed	50	mm/sec
Bed temperature	50	°C
Building orientation	Flat	-
Raster Angle	90°	-

Table 3: Constant process parameters

2.3 Sample Preparation

All samples are prepared according to ASTM 638D standard for tensile testing. Geometry is generated on solid works according to standards, as shown in figure 12. The solid works files are then converted to STL format, and g-codes are generated on Ultimaker Cura according to printing parameters.

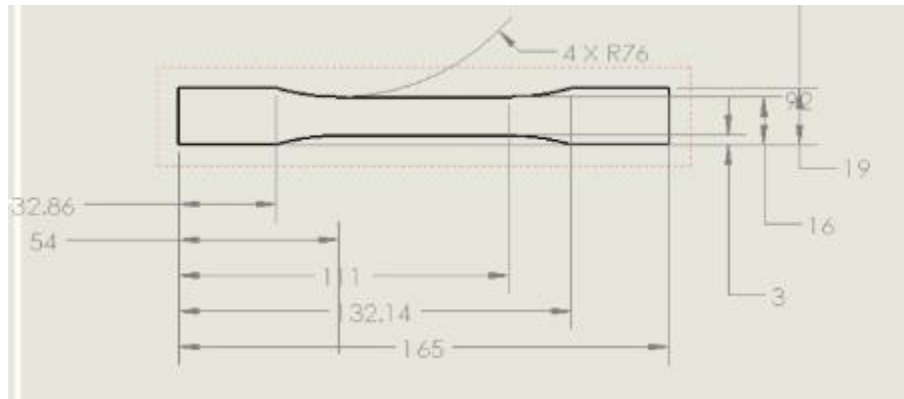


Figure 14: Solid works geometry of the specimen

In order to investigate all the varying factors DOE approach is used. It is the branch of statistics that helps to plan and organize the experiments. However, the disadvantage of using this approach is that by increasing the number of factors, the number of experiments also increases radically. To overcome this, Taguchi analysis is used to reduce the number of experiments. For statistical conclusion, the L_{18} array is used using Minitab software.

Sample No.	Layer thickness	Infill pattern	Infill percentage	Infill temperature	Heat treatment temperature
1	0.16	1	70	195	0
2	0.16	1	80	205	90
3	0.16	1	90	215	130
4	0.16	2	70	195	90
5	0.16	2	80	205	130
6	0.16	2	90	215	0
7	0.16	3	70	205	0
8	0.16	3	80	215	90
9	0.16	3	90	195	130

10	0.20	1	70	215	130
11	0.20	1	80	195	0
12	0.20	1	90	205	90
13	0.20	2	70	205	130
14	0.20	2	80	215	0
15	0.20	2	90	195	90
16	0.20	3	70	215	90
17	0.20	3	80	195	130
18	0.20	3	90	205	0

Table 4: Taguchi orthogonal array [Infill patterns: 1(octet), 2(Tri-hexagonal), (Gyriod)]

The solid works generated geometry is imported in Ultimaker Cura, and g-code files are generated for printing.

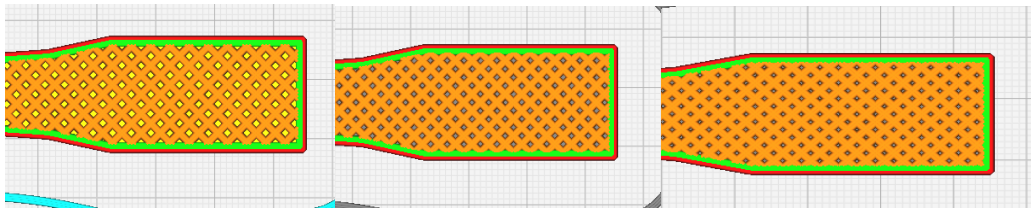


Figure 15: Octet infill pattern with 70, 80 and 90% infill density

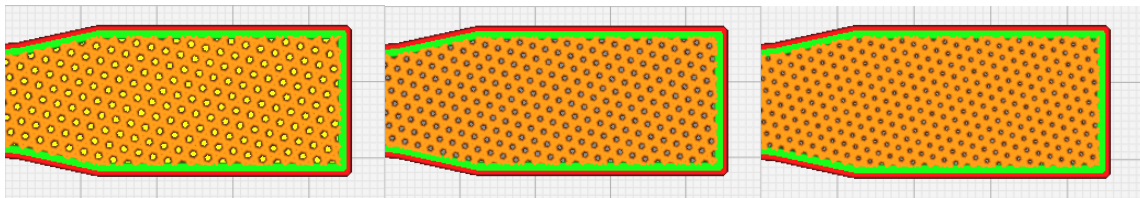


Figure 16: Tri-hexagonal infill pattern with 70, 80, and 90% infill density

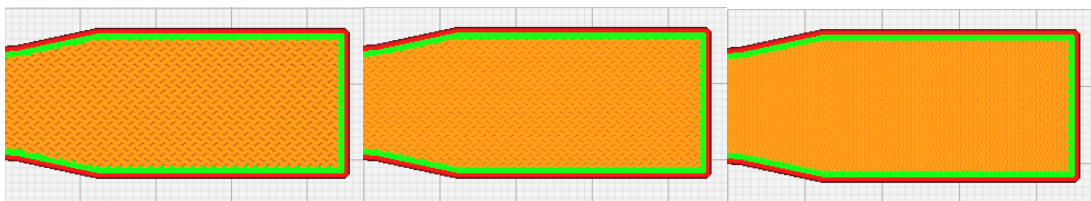


Figure 17: Gyroid infill pattern with 70, 80 and 90% infill density

The number of top/bottom layers for samples with 0.16mm layer thickness is 8, and the outer layer thickness is 0.80mm. The outer layer is of a rectilinear pattern. For a layer thickness of

0.20mm, the number of top/bottom layers is 8, and its thickness is 0.80mm. A total of 36 samples are generated, 2 for each set.

2.4 Orthogonal Array Experiment:

To examine the effect of the factors mentioned, a Taguchi L18 orthogonal array design was utilized. The objective of the study was to evaluate the tensile strength, which was used as the response parameter. The ultimate aim of the study was to achieve the maximum response values possible. A statistical program called Minitab was used to create the experimental matrix shown in Table 4.

2.5 Annealing:

Heat treatment known as annealing is frequently used to change the chemical or physical characteristics of materials like metals or polymers. This procedure is used to increase the material's hardness, ductility, or toughness. The material is heated to a high temperature, maintained there for a predetermined amount of time, and then progressively cooled to normal temperature during the annealing process. To provide the material the necessary qualities, cooling and heating processes are carefully regulated.

Commonly used to change the chemical or physical characteristics of materials like metals or polymers is the heat treatment procedure known as annealing. When annealing PLA, the PLA sample is heated above its glass transition temperature, which is generally approximately 60°C. Several techniques, including the use of a heat gun, oven, or furnace, can be used to conduct the annealing. An oven used for drying was used to carry out the annealing procedure for the present study. The samples with the numbers 2, 4, 8, 12, 15, and 16 were annealed at 90°C for an hour, whereas the samples with the numbers 3, 5, 9, 10, 13, and 17 were annealed at 130°C for the same amount of time. It's important to point out that the annealing temperature and time were chosen in consideration of the glass transition temperature and the unique material characteristics of the PLA samples. Each sample set is annealed for an hour at its given temperature. This carefully controlled annealing process was performed to modify the material's properties, particularly to enhance its toughness, ductility, and hardness. The use of a drying oven in this

study offers an efficient and reliable way to anneal PLA samples, making it an ideal method for use in similar studies.

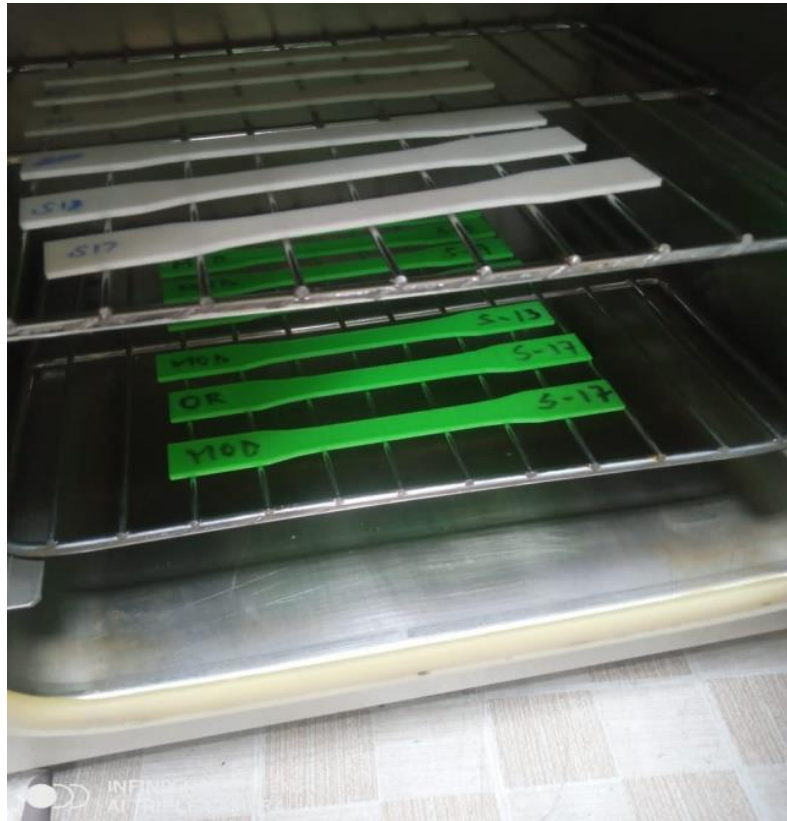


Figure 18: Samples placed in an oven for annealing

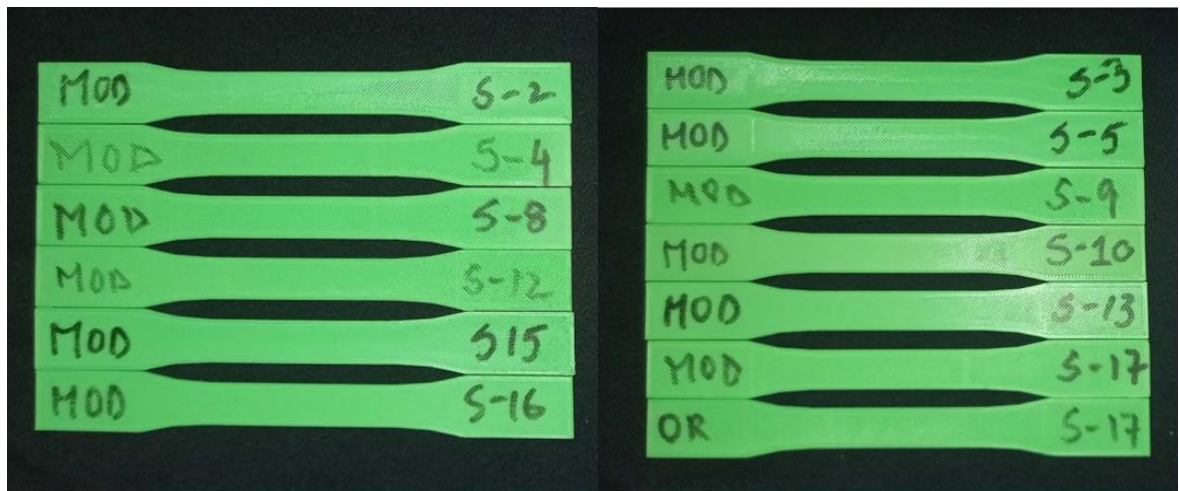


Figure 19: (a) Samples annealed at 90°C, (b) Samples annealed at 130°C

2.6 Tensile Testing

To conduct a tensile test on samples, a universal testing machine (UTM) is utilized. In this case, a SHIMADZU UTM with a maximum load cell capacity of 50kN and jaws that can open up to 7.0mm is employed. The tensile testing is performed using a 1000N load cell, and the crosshead speed is set to 1mm/min. The samples being tested have a length of 60mm, width of 13mm, and thickness of 3.2mm, and all the tests are carried out at room temperature.



Figure 20: Tensile test of a specimen

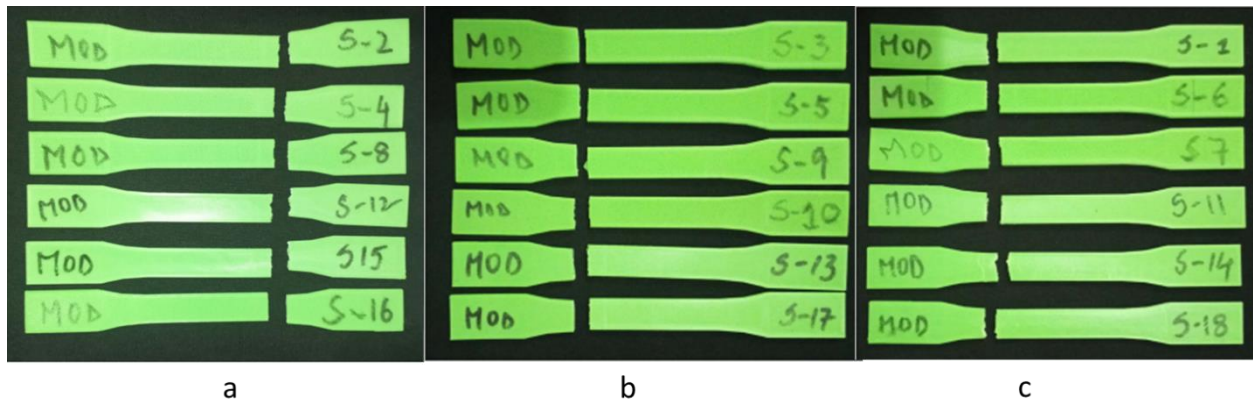


Figure 21: (a) 90°C annealed specimen after tensile test, (b) 130°C annealed specimen after tensile test, (c) un-annealed specimen after tensile test

Both annealed and unannealed samples that were put through a tensile test on the universal testing machine (UTM) are shown in Figure 23. It was also observed that both samples exhibited brittle behavior during the test as they broke suddenly and with little warning. This brittleness is

a result of the relatively low degree of deformation that the samples underwent during testing, which caused them to fail quickly without significant plastic deformation.

CHAPTER 3: RESULTS AND DISCUSSION

3.1 Tensile Test Results of Taguchi Matrix:

Table 5 provides a summary of the tensile test outcomes for each set of Taguchi orthogonal L18 array. The ultimate tensile strength (maximum stress) and strain percentage for each specimen are shown in the table. It is clear that sample number 18 has the highest ultimate tensile strength, while sample number 10 has the lowest.

Sample No.	Maximum Stress (MPa)	Strain Percentage
S1	26.68	2.98361
S2	32.7097	3.285
S3	28.5947	2.584
S4	29.2335	2.651
S5	22.5	2.31806
S6	25.1599	3.8001
S7	28.6991	3.1919
S8	30.1991	2.961
S9	29.8061	3.5475
S10	15.1254	1.6868
S11	24.0805	3.4151
S12	23.5142	2.0727
S13	20.3396	2.491
S14	23.6384	3.1444
S15	25.3974	2.8072
S16	27.6874	2.8049
S17	26.6075	2.945
S18	34.641	3.98339

Table 5: Experimental results of samples for Taguchi L18 Array

3.2 Signal-to-Noise Ratio (S/N):

By calculating the S/N ratio for each printing parameter, the impact of the specified printing parameters on the chosen response (maximum stress and strain %) was evaluated. When different printing parameter combinations are utilized, the signal-to-noise ratio—which is a log

function of the desired output—shows the degree of dispersion with relation to the anticipated response. When the ratio is large, the dispersion is minimal. Data analysis and outcome predicting are made easier by the signal-to-noise ratio. The findings of the tensile test were looked at to see how printing factors affected them. As stated in Table 4, the outcomes were then converted into the matching signal-to-noise ratio. Large is better was the standard for the S/N ratio.

Response Table for Signal-to-Noise Ratios

Larger is better

Level	LayerHeight	Infill Pattern	Infill %age	Infill Temperature	Heat Treat Temperature
1	28.95	27.77	27.60	28.59	28.60
2	27.61	27.69	28.42	28.48	28.93
3		29.40	28.82	27.78	27.32
Delta	1.34	1.71	1.22	0.82	1.61
Rank	3	1	4	5	2

Table 6: The S/N ratio analysis for tensile test result

Delta shows the significance of printing parameters. The highest value of delta is 1.71 for the infill pattern, which means it is the most significant parameter and ranked first. The maximum effectiveness ranks were determined using the highest and lowest average response values for each component, and delta values were used to show the difference (scatter) between those values.

Response Table for Means

Level	Layer Height	Infill Pattern	Infill %age	Infill Temperature	Heat Treat Temperature
1	28.18	25.12	24.63	26.97	27.15
2	24.56	24.38	26.62	27.07	28.12
3		29.61	27.85	25.07	23.83

Delta	3.62	5.23	3.22	2.00	4.29
Rank	3	1	4	5	2

Table 7: Response table for means

The graphical data clearly demonstrates that mean S/N ratio values decrease as layer thickness increases. But for infill patterns, the mean S/N ratio first falls and then rises. The gyroid infill pattern had the highest value, whereas the tri-hexagonal pattern had the lowest value. The S/N ratio drops when the printing temperature is raised, and annealing works best at 90°C. The poorest results come after annealing at 130°C. These results can be seen in figure 24.

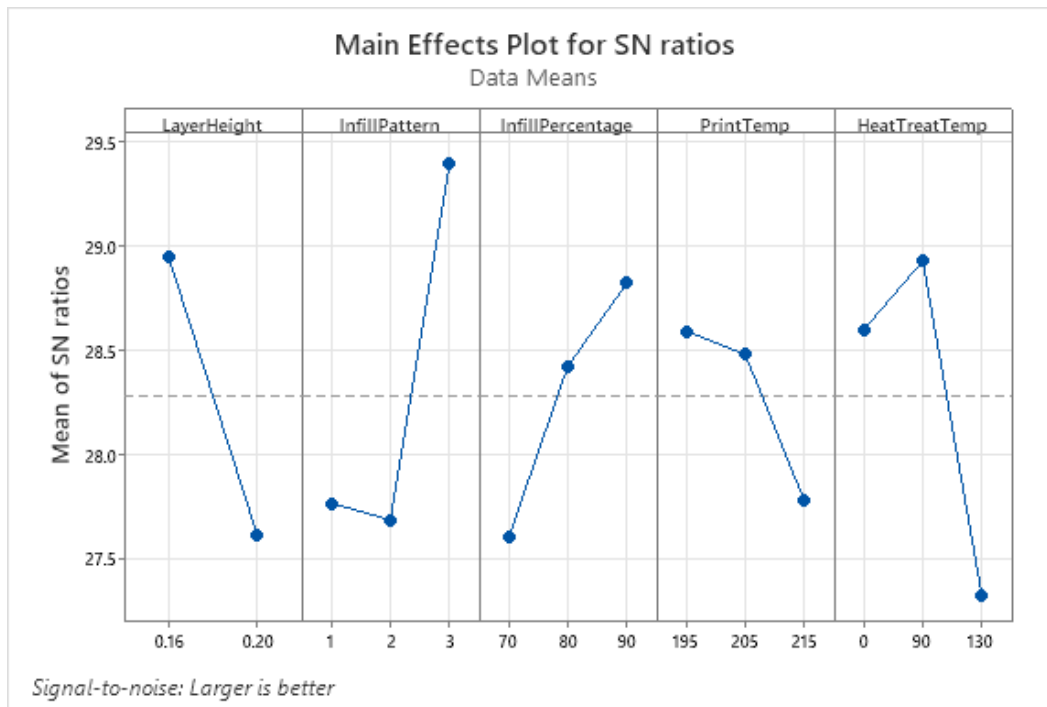


Figure 22: Plot of S/N ratio for UTS responses

Similarly, a response table for means and plot was also generated, which shows similar results as a signal to noise ratio plot with one exception. The best results can be observed when the printing temperature is 205°C.

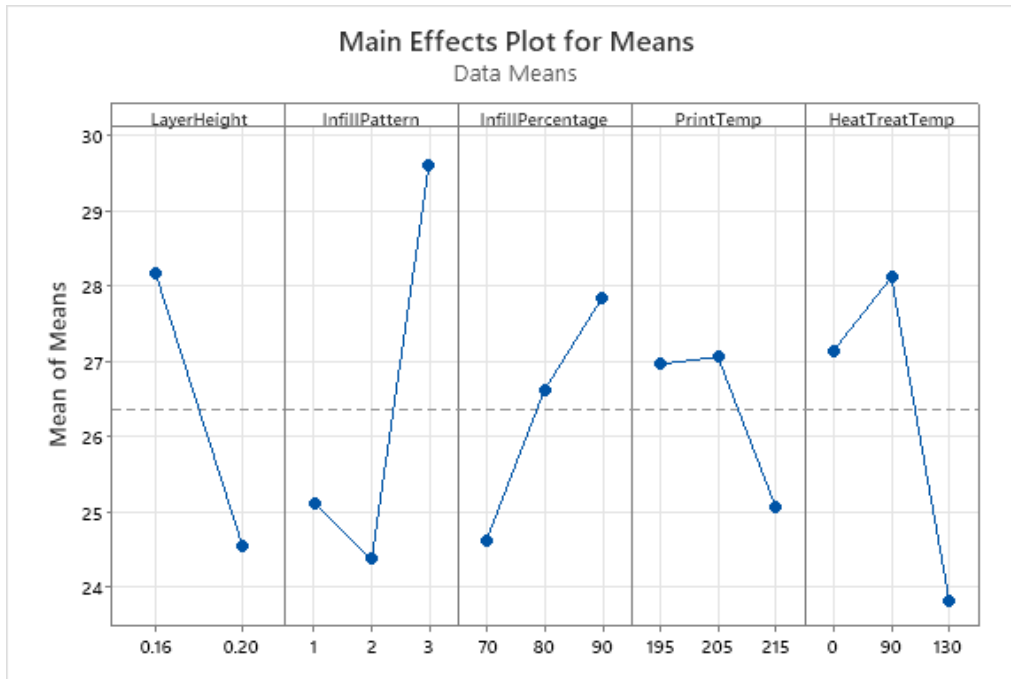


Figure 23: Plot of means for UTS responses

Similarly, strain percentage, S/N ratio, and means values are calculated using Taguchi analysis. It is evident from table 8 that for strain percentage most important factor while printing PLA specimens is post-heat treatment, and layer height is the least significant parameter.

Response Table for Signal-to-Noise Ratios

Larger is better

Level	Layer height	Infill Pattern	Infill Percentage	Infill Temperature	Heat Treatment
1	9.550	8.269	8.245	9.663	10.633
2	8.748	9.035	9.510	8.996	8.747
3		10.142	9.690	8.787	8.066
Delta	0.802	1.874	1.445	0.876	2.566
Rank	5	2	3	4	1

Table 8: S/N ratio analysis for strain percentage

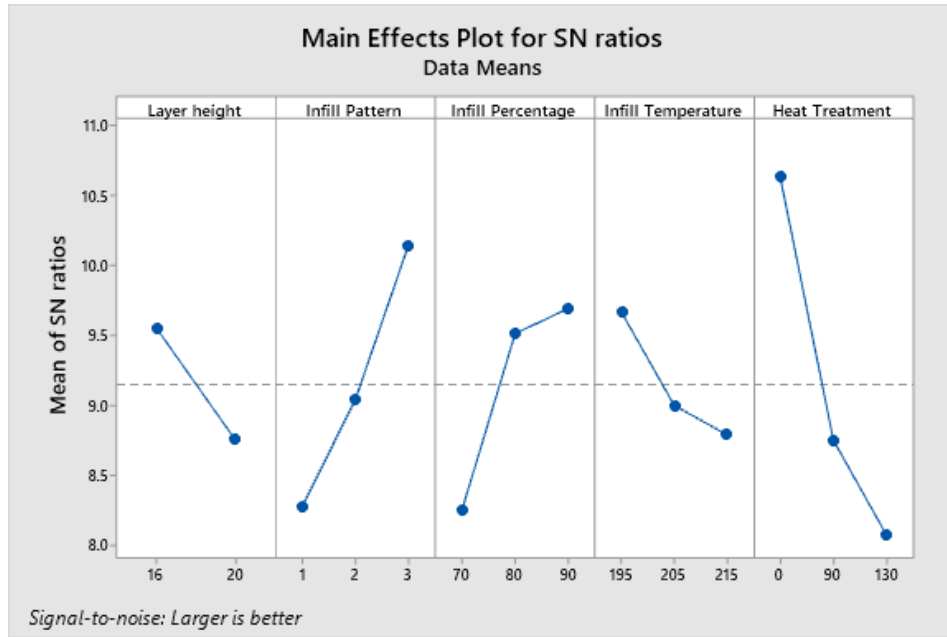


Figure 24: Plot of S/N ratio for Strain percentage responses

The graphical data in figure 26 makes it crystal evident that while the strain percentage falls as layer thickness increases, it rises as the infill percentage does. The worst strain percentage value is displayed by octet infill patterns, whereas gyroid infill patterns provide the best values. The strain percentage reduces as the printing temperature is raised. The best strain percentage values typically come from specimens that haven't been annealed.

3.3 Estimation of optimum parameters:

Based on S/N ratio analysis and the Main effect plot of the mean and S/N ratio, it appears that layer thickness of 0.16mm, gyroid infill pattern, 90% infill density, printing temperature of 195°C, and post-treatment samples annealed at 90°C can maximize tensile strength. The sample should not be annealed and should have a layer thickness of 0.16, a gyroid infill pattern, an infill density of 90%, and a printing temperature of 195°C to get the best stain percentage.

3.4 Prediction of the Optimum Parameter by Regression equation:

Regression equation has the advantage of being able to forecast future responses in addition to determining how the response changes as the values of the process parameters are altered. Regression prediction is the process of estimating the value of a single variable from the

presumptive values of other related input variables. The mean UTS was compared to the selected process parameters to create a fit regression equation. The equation in figure 27 describes the regression model of the presented case.

$$UTS = 74.7 - 226.2 \times h - 16.88 \times p + 0.1020 \times f - 0.0950 \times T - 0.000909 \times T^2 + 106.2 \times h \times p - 1.046 \times h \times T$$

Equation 1: Regression equation for UTS

In this equation h represents the layer height, p represents the infill pattern, f represents the infill percentage, T represents the heat treat temperature.

A model summary can be seen in table 9. The R-square term is important, and it should be greater than 70%. An R-square value greater than 70% is good to be accepted. For this equation of tensile strength R-square value is 82.85%

Model Summary

S	R-sq	R-sq(adj)	R-sq(pred)
2.60679	82.85%	67.60%	39.09%

Table 9: Regression model summary

The coefficient table can also be obtained from Minitab. It shows all coefficients in the regression equation. In this table, the p-value is very important. Against each parameter, it should be less than 0.05 for the parameter to be affecting the results significantly.

Coefficients

Term	Coef	SE Coef	T-Value	P-Value	VIF
Constant	74.7	22.8	3.27	0.010	
Layer height	-226.2	93.3	-2.42	0.038	9.22
Infill pattern	-16.88	6.81	-2.48	0.035	82.00
Infill density	0.1020	0.0832	1.23	0.251	1.22
Infill temperature	-0.0950	0.0753	-1.26	0.239	1.00
Heat treatment	0.281	0.122	2.31	0.047	116.26
Heat treatment*Heat treatment	-0.000909	0.000371	-2.45	0.037	17.35
Layer height*Infill pattern	106.2	37.6	2.82	0.020	88.00
Layer height*Heat treatment	-1.046	0.624	-1.67	0.128	102.35

Table 10: Coefficients table of the regression equation for UTS

It can be seen from the table that layer height, infill pattern, and heat treatment temperature are significant parameters when calculating tensile strength. Similarly, the regression equation for strain percentage was obtained through Minitab.

Regression Equation for Strain percentage

$$\text{Strain \%} = 6.23 + 0.0014 \times T - 0.0114 \times T_i + 0.0215 \times f - 0.999 \times f + 15.3 \times h - 0.0000024 \times T^2 - 0.0601 \times T \times h + 7.13 \times f \times h$$

Equation 2: Regression equation for strain percentage

In this equation T_i is the infill temperature. Table 11 shows that no parameter is significant while calculating strain percentage as the p-value is not less than 0.05 for either parameter. The R-square value is 80.39% which is greater than 70% which makes this model acceptable.

Coefficients

Term	Coef	SE Coef	T-Value	P-Value	VIF
Constant	6.23	3.11	2.00	0.076	
Heat Treatment	0.0014	0.0166	0.08	0.935	116.26
Infill Temperature	-0.0114	0.0103	-1.11	0.296	1.00
Infill Percentage	0.0215	0.0113	1.89	0.091	1.22
Infill Pattern	-0.999	0.930	-1.07	0.310	82.00
Layer height	-15.3	12.7	-1.20	0.259	9.22
Heat Treatment*Heat Treatment	0.000024	0.000051	0.47	0.650	17.35
Heat Treatment*Layer height	-0.0601	0.0852	-0.71	0.498	102.35
Infill Pattern*Layer height	7.13	5.13	1.39	0.198	88.00

Table 11: Coefficient table of the regression equation for stain %

Model Summary

S	R-sq	R-sq(adj)	R-sq(pred)
0.355625	80.39%	62.96%	25.01%

Table 12: Regression model summary for strain % age

3.5 Analysis of Variance (ANOVA)

The following table shows the optimal settings for ultimate tensile strength and stain percentage, according to the analysis that has been done.

Parameter	Level	
	For maximum stress	For maximum strain % age

Layer Height	0.16	0.16
Infill density	90%	90%
Infill pattern	Gyroid	Gyroid
Infill temperature	195°C	195°C
Heat treat temperature	90°C	0°C

Table 13: Optimum parameters

To determine the relevance of each process parameter and its effect on the predefined outputs, a statistical tool must be used. This is due to the Taguchi experimental method's inability to illuminate the precise mechanisms by which each process parameter influences the desired outcomes, such as UTS and strain%age. The Analysis of Variance (ANOVA) approach was used to specifically quantify each parameter's usefulness in order to solve this issue. ANOVA may also calculate the proportion of the response that each particular process parameter contributes. The importance of each process parameter was evaluated using the comparison of f and p values, and the analysis was performed with a 95% confidence level. Higher f-valued process parameters are thought to have a more substantial impact on process responses. A further measure used to assess the relevance of process parameters is the p-value, with lower p-values denoting a higher effect on the response. In general, if the p-value is less than 0.05, a parameter has a significant effect on the process response. Additionally, Table 10—which lists the outcomes of the ANOVA analysis for mean UTS—calculated and displayed the% contribution of each process parameter.

Analysis of Variance

Source	DF	Adj SS	Adj MS	F-Value	P-Value
Regression	8	295.43	36.928	5.43	0.010
Heat Treatment	1	36.11	36.106	5.31	0.047
Infill Temperature	1	10.83	10.830	1.59	0.239
Infill Percentage	1	10.22	10.218	1.50	0.251
Infill Pattern	1	41.68	41.684	6.13	0.035
Layer height	1	39.94	39.943	5.88	0.038
Heat Treatment*Heat Treatment	1	40.83	40.833	6.01	0.037
Heat Treatment*Layer height	1	19.06	19.063	2.81	0.128
Infill Pattern*Layer height	1	54.17	54.170	7.97	0.020
Error	9	61.16	6.795		
Total	17	356.58			

Table 14: Analysis of Variance (Maximum stress)

According to the analysis, UTS is most affected by heat treatment, layer height, and infill pattern. So, in this scenario, these are the most important printing factors. 10.12% of the output response is affected by heat treatment. Only 3.03 percent of output is influenced by infill temperature. Infill pattern, Infill percentage, and layer height each contribute 11.68%, 2.8%, and 11.20%, respectively, to the output response, or UTS. This leads to the conclusion that Infill patterns affect UTS the most, whilst Infill percentage has the least impact. Table 14 shows each process parameter's contribution to strain percentage.

Analysis of Variance

Source	DF	Adj SS	Adj MS	F-Value	P-Value
Regression	8	4.66549	0.583187	4.61	0.017
Heat Treatment	1	0.00089	0.000894	0.01	0.935
Infill Temperature	1	0.15600	0.156000	1.23	0.296
Infill Percentage	1	0.45313	0.453130	3.58	0.091
Infill Pattern	1	0.14614	0.146137	1.16	0.310
Layer height	1	0.18336	0.183362	1.45	0.259
Heat Treatment*Heat Treatment	1	0.02781	0.027807	0.22	0.650
Heat Treatment*Layer height	1	0.06301	0.063007	0.50	0.498
Infill Pattern*Layer height	1	0.24393	0.243932	1.93	0.198
Error	9	1.13822	0.126469		
Total	17	5.80371			

Table 15: Analysis of Variance (strain % age)

According to ANOVA, no parameter has a significant impact on strain percentage because no value of p is less than 0.05 for any parameter.

3.6 Validation Test:

The next step was to conduct a confirmatory test using the best parameters after choosing the optimized printing parameters. For this purpose, 2 additional samples were made. Tensile tests on sample S21 produced the highest UTS. The highest UTS that was attained, 37.15MPa, was extremely close to the value anticipated by the UTS regression equation. Similar to strain percentage, the sample produced using the best printing parameters for stain percentage resulted in a maximum value of 7.28%. The testing findings validated the model's applicability and efficacy in choosing the best PLA 3D printing parameters.

CHAPTER 4: CONCLUSION AND FUTURE WORK

In this study, Taguchi statistical analysis was used to determine the best process parameters to maximize the tensile strength of 3D-printed PLA. With regard to "Layer height," "Infill density," "Infill pattern," "Printing temperature," and "Annealing temperature," mixed levels of the five most effective process parameters were used. Along with quantifying each parameter's contribution, the most significant and least significant parameters were identified. On the basis of analytical, numerical, and experimental analyses, the following findings have been drawn.

1. The Taguchi Design of Experiment technique can effectively be used to optimize the printing settings for PLA samples when printing them in a 3D printer.
2. Signal to noise ratio reveals optimum printing parameters for maximum. When the values of "Layer height," "Infill density," "Infill pattern," "printing temperature," and "annealing temperature" are 0.16 mm, 90%, gyroid, 195°C, and 90°C, respectively, the maximum tensile strength can be achieved. The UTS that was feasible was 37.15.
3. S/N analysis revealed that the values of "Layer height," "Infill density," "Infill pattern," "printing temperature," and "annealing temperature" should be 0.16 mm, 90%, gyroid, 195°C, and 0°C, respectively, to achieve the maximum strain percentage. The elongation percentage that was feasible was 7.28%.
4. According to an ANOVA analysis, "Infill pattern" contributed 11.68% to the 3D printed PLA's tensile strength, followed by "Layer height" and "Heat treatment temperature," which contributed 11.20% and 10.12%, respectively.
5. According to Taguchi's Analysis, Infill Pattern is the most important factor influencing the tensile strength of 3D printed PLA, while Heat Treatment Temperature is placed second. For the staining percentage of 3D printed PLA, Heat Treatment Temperature is the factor with the maximum delta (standard deviation).

4.1 FUTURE WORK:

Add reinforcing fibers or particles: To increase the strength of PLA, various reinforcing fibers or particles, such as carbon fibers, glass fibers, or metal particles, may be added. The tensile strength of 3D printed components can be considerably increased by these additions.

Post-processing methods: A variety of post-processing methods can be employed to increase the strength of PLA used in 3D printing. For instance, the part's crystalline structure and strength can be improved by annealing it by heating it in an oven, as seen. The surface of the part may also benefit from a coating or treatment to increase its resistance to wear and tear.

Acetone smoothing: Acetone vapor can be used to smooth the PLA component's surface, which can strengthen the part by strengthening the interlayer bonds. The interlayer bonding can also be strengthened, and the surface of the printed object can be polished mechanically using sandpaper, polishing chemicals, or a tumbler.

Epoxy coating: Epoxy resin can be applied to the printed item to add additional strength and stiffness.

UV post-curing: Because some 3D printing resins are UV light sensitive, post-curing the printed object under UV light can increase the material's tensile strength and toughness.

It is important to keep in mind that each of these methods could have disadvantages and restrictions, so it's crucial to think about the particular needs of your project and choose the strategy that will work the best for you. Moreover, the type and brand of PLA filament used for printing might have an impact on each technique's efficacy.

REFERENCES

1. Alafaghani, A.a., et al., *Experimental Optimization of Fused Deposition Modelling Processing Parameters: A Design-for-Manufacturing Approach*. Procedia Manufacturing, 2017. **10**: p. 791-803.
2. Hsueh, M.H., et al., *Effect of Printing Parameters on the Tensile Properties of 3D-Printed Polylactic Acid (PLA) Based on Fused Deposition Modeling*. Polymers (Basel), 2021. **13**(14).
3. Algarni, M., *The Influence of Raster Angle and Moisture Content on the Mechanical Properties of PLA Parts Produced by Fused Deposition Modeling*. Polymers (Basel), 2021. **13**(2).
4. Jayanth, N., et al., *Effect of heat treatment on mechanical properties of 3D printed PLA*. J Mech Behav Biomed Mater, 2021. **123**: p. 104764.
5. *3D printing blog*. 2014; Available from: <https://www.valeriomarcotuli.com/3d-printing-setting-parameters/>.
6. *Filaments and chips*. 2022; Available from: <https://filnchips.com/pages/3d-printing-parameters>.
7. Marcotuli, V. *3D printing setting parameters*. 2021; Available from: <https://www.valeriomarcotuli.com/3d-printing-setting-parameters/>.
8. Creation, C. *3D Printing PETG Filament: Ideal Bed Temp & Print Settings*. 2022; Available from: <https://clevercreations.org/petg-temperature-bed-temp-print-settings/#:~:text=To%203D%20print%20well%20with%20PETG%20filament%2C%20you,for%20the%20rest%20of%20the%20print%20if%20needed>.
9. Bros., M. *What is Infill in 3D Printing?* 2022; Available from: https://themachinebros.com/what-is-infill-in-3d-printing/#Internal_Fill_Pattern.
10. Prabhakar, M.M., *A short review on 3D printing methods, process parameters, and materials*. Science Direct, 2021. **45**: p. 7.

11. Ganeshkumar, D.K., U. Magarajan, S. Rajkumar, B. Arulmurugan, Shubham Sharma, Changhe Li, R. A. Ilyas, Mohamed Fathy Badran, *Investigation of Tensile Properties of Different Infill Pattern*. MDPI, 2022: p. 11.
12. Pearce, B.W.J.M., *The Effects of PLA Color on Material Properties of 3-D*. 2015: p. 15.
13. Muammel M. Hanona, b., *, József Dobosa, *The influence of 3D printing process parameters on the mechanical*. Procedia Manufacturing, 2021: p. 244–249.
14. Kyoung-SU Seol, P.Z., Byoung-Chul Shin, Sung-Uk Zhang, *Infill Print Parameters for Mechanical Properties of 3D Printed PLA Parts*. Journal of the Korean Society of Manufacturing Process Engineers, 2018: p. 8.
15. Mohammad Reza Khosravani, F.B., Majid R.Ayatollahi & Tamara Reinicke, *Characterization of 3D-printed PLA parts with different raster orientations and printing speeds*. Scientific reports, 2022: p. 9.
16. Chamil Abeykoon, P.S.-A., Anura Fernando, *Optimization of fused deposition modeling parameters for improved PLA and ABS 3D printed structures*. International Journal of Lightweight Materials and Manufacture, 2020: p. 14.
17. Antonio Lanzotti, M.G., Gabriele Staiano and Massimo Martorelli, *The impact of process parameters on mechanical properties of parts fabricated in PLA with an open-source 3-D printer*. Rapid Prototyping Journal, 2015: p. 19.
18. Dave, S.R.R.H.K., *Analysis of tensile strength of a fused filament fabricated PLA part using an open-source 3D printer*. The International Journal of Advanced Manufacturing, 2019: p. 12.
19. K.N. Gunasekaran, V.A., C.B. Muthu Kumaran, K. Madhankumar, S. Pradeep Kumar, *Investigation of mechanical properties of PLA printed materials under varying infill density*. Materials Today: Proceedings, 2020: p. 8.
20. Marzio Grasso, L.A.a.P.R.-H., *Effect of temperature on the mechanical properties of 3D-printed PLA tensile specimens*. Rapid Prototyping Journal, 2018: p. 11.
21. Radosław A. Wach, P.W., and Agnieszka Adamus-Włodarczyk, *Enhancement of Mechanical Properties of FDM-PLA Parts via Thermal Annealing*. Macromolecular materials and engineering 2018: p. 9.
22. Y. Song, Y.L., W. Song, K. Yee, K.-Y. Lee and V.L. Tagarielli, *Measurements of the mechanical response of unidirectional 3D-printed PLA*. Materials & Design, 2017: p. 36.

23. Vikas Chandran, K.F., Jordan Kalman, Habiba Bougherara, *A comparative study of the tensile properties of compression molded and 3D printed PLA specimens in dry and water saturated conditions*. Journal of Mechanical Science and Technology, 2021: p. 8.
24. Pushendra Yadav, A.S., Rahul Swarup Sharma, *Strength and Surface Characteristics of FDM-Based 3D Printed PLA Parts for Multiple Infill Design Patterns*. J. Inst. Eng. India Ser. C, 2020: p. 11.
25. M. Kamaalm, M.A., H. Rastogi, N. Bhardwaj, A. Rahaman, *Efect of FDM process parameters on mechanical properties of 3D-printed carbon fiber–PLA composite*. Progress in Additive Manufacturing, 2020: p. 7.
26. Harsh Chokshi, D.B.S., Kaushik M. Patel & Shashikant J. Joshi, *Experimental investigations of process parameters on mechanical properties for PLA during processing in FDM*. Advances in Materials and Processing Technologies, 2021: p. 15.
27. Giri, J., et al., *Effect of process parameters on mechanical properties of 3d printed samples using FDM process*. Materials Today: Proceedings, 2021. **47**: p. 5856-5861.
28. Rismalia, M., et al., *Infill pattern and density effects on the tensile properties of 3D printed PLA material*. Journal of Physics: Conference Series, 2019. **1402**(4).
29. Pandzic, A., D. Hodzic, and A. Milovanovic, *Effect of Infill Type and Density on Tensile Properties of PLA Material for FDM Process*, in *Proceedings of the 30th International DAAAM Symposium 2019*. 2019. p. 0545-0554.
30. Chacón, J.M., et al., *Additive manufacturing of PLA structures using fused deposition modelling: Effect of process parameters on mechanical properties and their optimal selection*. Materials & Design, 2017. **124**: p. 143-157.
31. Derise, Mohammad & Zulkharnain, Azham. (2021). *Effect of Infill Pattern and Density on Tensile Properties of 3D Printed Polylactic acid Parts via Fused Deposition Modeling (FDM)*. International Journal of Mechanical & Mechatronics Engineering. 20. 54-62. .pdf.
32. Bhandari, S., R.A. Lopez-Anido, and D.J. Gardner, *Enhancing the interlayer tensile strength of 3D printed short carbon fiber reinforced PETG and PLA composites via annealing*. Additive Manufacturing, 2019. **30**.
33. Ayatollahi, M.R., et al., *The influence of in-plane raster angle on tensile and fracture strengths of 3D-printed PLA specimens*. Engineering Fracture Mechanics, 2020. **237**.
34. Muammel M. Hanon, József Dobos, László Zsidai, *The influence of 3D printing process parameters on the mechanical performance of PLA polymer and its correlation with*

- hardness, Procedia Manufacturing, Volume 54, 2021, Pages 244-249, ISSN 2351-9789, <https://doi.org/10.1016/j.promfg.2021.07.038>. hanon2021.*
35. Behzadnasab, M., et al., *Effects of processing conditions on mechanical properties of PLA printed parts*. Rapid Prototyping Journal, 2019. **26**(2): p. 381-389.
 36. Liao, Y., et al., *Effect of Porosity and Crystallinity on 3D Printed PLA Properties*. Polymers (Basel), 2019. **11**(9).
 37. Waseem, M., et al., *Multi-Response Optimization of Tensile Creep Behavior of PLA 3D Printed Parts Using Categorical Response Surface Methodology*. Polymers (Basel), 2020. **12**(12).
 38. Heidari-Rarani, M., et al., *Optimization of FDM process parameters for tensile properties of polylactic acid specimens using Taguchi design of experiment method*. Journal of Thermoplastic Composite Materials, 2020. **35**(12): p. 2435-2452.
 39. Leite, Marco & fernandes, João & Deus, Augusto & Reis, Luis & Vaz, M.F.. (2018). *STUDY OF THE INFLUENCE OF 3D PRINTING PARAMETERS ON THE MECHANICAL PROPERTIES OF PLA..pdf*.
 40. Tymrak, B.M., M. Kreiger, and J.M. Pearce, *Mechanical properties of components fabricated with open-source 3-D printers under realistic environmental conditions*. Materials & Design, 2014. **58**: p. 242-246.
 41. Ayrilmis, N., et al., *Effect of printing layer thickness on water absorption and mechanical properties of 3D-printed wood/PLA composite materials*. The International Journal of Advanced Manufacturing Technology, 2019. **102**(5-8): p. 2195-2200.
 42. Liu, Z., et al., *A critical review of fused deposition modeling 3D printing technology in manufacturing polylactic acid parts*. The International Journal of Advanced Manufacturing Technology, 2019. **102**(9-12): p. 2877-2889.
 43. Al Khawaja, Huda & Alabdouli, Haleimah & Alqaydi, Hend & Mansour, Aya & Ahmed, Waleed & Jassmi, Hamad. (2020). *Investigating the Mechanical Properties of 3D Printed Components*. 1-7. [10.1109/ASET48392.2020.9118307](https://doi.org/10.1109/ASET48392.2020.9118307). pdf>.
 44. Czyzewski, P., et al., *Influence of Extruder's Nozzle Diameter on the Improvement of Functional Properties of 3D-Printed PLA Products*. Polymers (Basel), 2022. **14**(2).
 45. Nugroho, A., et al., *Effect of layer thickness on flexural properties of PLA (PolyLactid Acid) by 3D printing*. Journal of Physics: Conference Series, 2018. **1130**.

46. Vinoth Babu, N., et al., *Influence of slicing parameters on surface quality and mechanical properties of 3D-printed CF/PLA composites fabricated by FDM technique*. *Materials Technology*, 2021. **37**(9): p. 1008-1025.
47. Chalgham, A., A. Ehrmann, and I. Wickenkamp, *Mechanical Properties of FDM Printed PLA Parts before and after Thermal Treatment*. *Polymers (Basel)*, 2021. **13**(8).

CERTIFICATE OF COMPLETENESS

It is hereby certified that the dissertation submitted by NS Muhammad Uzair Nadeem, Reg No. **00000330022**, Titled: ***Effect of printing parameters on mechanical characteristics of 3D printed PLA***, has been checked/reviewed, and its contents are complete in all respects.

Supervisor's Name: **Dr. Hasan Aftab Saeed**

Signature: _____

Date: _____